Forschungszentrum Karlsruhe
in der Helmholtz-Gemeinschaft

Wissenschaftliche Berichte
FZKA 7086
SAM-LACOMERA-D01

Analytical Support for the Preparation of Bundle Test QUENCH-10 on Air Ingress

C. Homann, W. Hering, J. Birchley, T. Haste

Institut für Reaktorsicherheit
Programm Nukleare Sicherheitsforschung

Juli 2005

Forschungszentrum Karlsruhe

in der Helmholtz-Gemeinschaft

Wissenschaftliche Berichte

FZKA 7086

SAM-LACOMERA-D01

Analytical Support for the Preparation of Bundle Test QUENCH-10 on Air Ingress

Ch. Homann, W. Hering,

J. Birchley[1], T. Haste[1]

Institut für Reaktorsicherheit

Programm Nukleare Sicherheitsforschung

[1]Paul Scherrer Institut, Villigen, Switzerland

Forschungszentrum Karlsruhe GmbH, Karlsruhe

2005

Impressum der Print-Ausgabe:

Als Manuskript gedruckt

Forschungszentrum Karlsruhe GmbH
Postfach 3640, 76021 Karlsruhe

Mitglied der Hermann von Helmholtz-Gemeinschaft
Deutscher Forschungszentren (HGF)

ISSN 0947-8620

urn:nbn:de:0005-070861

Abstract

Bundle test QUENCH-10 is dedicated to study air ingress with subsequent water quench during a supposed accident in a spent fuel storage tank. It was proposed by AEKI, Budapest, Hungary and was performed on 21 July 2004 in the QUENCH facility at Forschungszentrum Karlsruhe. Preparation of the test is based on common analytical work at Forschungszentrum Karlsruhe and Paul Scherrer Institut, Villigen, Switzerland, mainly with the severe accident codes SCDAP/RELAP5 and MELCOR, to derive the protocol for the essential test phases, namely pre-oxidation, air ingress and quench phase. For issues that could not be tackled by this computational work, suggestions for the test conduct were made and applied during the test. Improvements of the experimental set-up and the test conduct were suggested and largely applied. In SCDAP/RELAP5, an error was found: for thick oxide scales, the output value of the oxide scale is sensibly underestimated. For the aims of the test preparation, its consequences could be taken into account.

Together with the related computational and other analytical support by the engaged institutions the test is co-financed as test QUENCH-L1 by the European Community under the Euratom Fifth Framework Programme on Nuclear Fission Safety 1998 – 2002 (LACOMERA Project, contract No. FIR1-CT2002-40158).

Zusammenfassung

Analytische Unterstützung für die Vorbereitung des Bündeltests QUENCH-10 zum Lufteinbruch

Der Bündel-Versuch QUENCH-10 dient der Untersuchung eines Lufteinbruches mit nachfolgendem Abschrecken des Bündels mit Wasser in einem angenommenen Unfall in einem Lagerbecken für abgebrannte Brennelemente. Er wurde von AEKI, Budapest, Ungarn, vorgeschlagen und am 21. Juli 2004 in der QUENCH-Anlage im Forschungszentrum Karlsruhe durchgeführt. Analytische Arbeiten zur Festlegung der wichtigen Versuchsphasen Voroxidation, Lufteinbruch und Abschrecken beruhen auf einer gemeinsamen Arbeit des Forschungszentrums Karlsruhe und des Paul Scherrer Instituts, Villigen, Schweiz, vor allem mit den Rechenprogrammen SCDAP/RELAP5 und MELCOR zur Beschreibung von schweren Störfällen. Für Fragen, die nicht durch diese Rechnungen lösbar waren, wurden Vorschläge zur Versuchsdurchführung gemacht und im Versuch angewandt. Verbesserungen im experimentellen Bereich wurden vorgeschlagen und zu einem großen Teil umgesetzt. In SCDAP/RELAP5 wurde ein Programmfehler gefunden: bei großen Oxidschichtdicken wird der Ausgabewert der Oxidschichtdicke deutlich unterschätzt. Für die Belange der Testvorbereitung konnten seine Auswirkungen abgeschätzt werden.

Zusammen mit der zugehörigen analytischen Unterstützung durch die beteiligten Einrichtungen wurde er als Test QUENCH-L1 im 5. Rahmenprogramm der Euratom zur Sicherheit der Kernspaltung 1998 – 2002 (Projekt LACOMERA, Vertragsnummer FIR1-CT2002-40158) teilweise durch die Europäische Union finanziert.

TABLE OF CONTENTS

1 Introduction 1

2 Nuclear Scenario 2

3 Experimental Basis 4
3.1 Quench Facility 4
3.2 QUENCH Draft Test Protocol 7

4 FZK/IRS Calculations 8
4.1 General 8
4.2 Computational Basis 8
4.3 Modelling of the QUENCH Facility 8
4.4 FZK/IRS Calculations 10

5 Other Analytical Work at FZK/IRS 16
5.1 Oxide Scale in S/R5 16
5.2 Contributions to Experimental Issues 22

6 PSI Contributions 24
6.1 Introduction 24
6.2 Pre-oxidation and Air Ingress 27
6.3 Quench/Cool-Down 30
6.4 Oxidation 34
6.5 Code Comparison and Discussion of Uncertainties 37

7 End of Pre-Oxidation Phase 39

8 Joint Proposals for Final Test Protocol 41

9 Conclusions 42

10 Acknowledgement 44

11 References 45

TABLES

Tab. 5.1: Calculated and measured oxide scales at 8000 and 11000 s 16
Tab. 6.1: Typical power histories for S/R5 calculations 25
Tab. 6.2: Typical fluid flow histories for S/R5 calculations 26
Tab. 6.3: Details of oxidation modelling 26

FIGURES

Fig. 2.1: Spent fuel storage pool 3
Fig. 3.1: Main flow paths in the QUENCH facility 5
Fig. 3.2: Bundle cross section 6
Fig. 4.1: FZK: Modelling of the QUENCH facility with S/R5 9
Fig. 4.2: FZK: Survey of pre-test calculations (part 1) 12
Fig. 4.3: FZK: Survey of pre-test calculations (part 2) 13
Fig. 4.4: FZK: Time dependent results of final pre-test calculation 14
Fig. 4.5: FZK: Axial profiles for selected variables for final pre-test calculation 15
Fig. 5.1: FZK: Hydrogen generation in central rod, calculated with S/R5 and SVECHA 18
Fig. 5.2 FZK: Central rod results, calculated with S/R5 and SVECHA 19
Fig. 5.3: FZK: Axial profiles of clad data at 8000 s 20
Fig. 5.4: FZK: Axial profiles of clad data at 11000 s 21
Fig. 5.5: Current design for high temperature TCs 22
Fig. 6.1: PSI: MELCOR and S/R5 temperature histories, original specification 28
Fig. 6.2: PSI: Calculated peak reacted metal layer histories 28
Fig. 6.3: PSI: Effect of reduced heat transfer only 29
Fig. 6.4: PSI: Effect of reduced heat transfer and air oxidation 29
Fig. 6.5: PSI: MELCOR temperature histories, original and revised specification 30
Fig. 6.6: PSI: Temperature histories for different cooling methods after air ingress 31
Fig. 6.7: PSI: Comparison of helium cooling and water quench (MELCOR) 32
Fig. 6.8: PSI: S/R5 temperature histories for argon cooling at 30 g/s 32
Fig. 6.9: PSI: Quench front and collapsed water level for water quench at 50 g/s 33
Fig. 6.10: PSI: Quench front and collapsed water level for water quench at 20 g/s 33
Fig. 6.11: PSI: Remaining metallic in inner ring cladding for water quench at 20 g/s 34
Fig. 6.12: PSI: Hydrogen production for different cooling methods 35
Fig. 6.13: PSI: Hydrogen production for reflood at 20 g/s and 50 g/s 35
Fig. 6.14: PSI: Oxidised metal thickness for reflood at 50 g/s 36
Fig. 6.15: PSI: Oxidised metal thickness for reflood at 20 g/s 36
Fig. 7.1: Maximum oxide scale versus cumulated hydrogen generation 40

Abbreviations

AEKI	Atomic Energy Research Institute, Budapest, Hungary
AIT	Air Ingress Test
CODEX	Core Degradation Experiment
CORA	Complex Out-of-pile Rod bundle Assembly
FRAP-T	Fuel Rod Analysis Program - Transient
FZK	Forschungszentrum Karlsruhe, Germany
IMF	Institute for Material Research at FZK
ISP	OECD International Standard Problem
IRS	Institute for Reactor Safety at FZK
JRC	Joint Research Centre, Ispra
LACOMERA	Large scale experiments on core degradation, melt retention and coolability
LWR	Light Water Reactor
MS	Mass spectrometer
NPP	Nuclear Power Plant
OECD	Organization for Economic Co-operation and Development
OPSA	Oxidation Phenomena in Severe Accidents
PSI	Paul Scherrer Institut, Villigen, Switzerland
PWR	Pressurized Water Reactor
RELAP5	formerly: Reactor Excursions and Leak Analysis Program, now: Reactor Leak and Analysis Program
SCDAP	Severe Core Damage Analysis Package
SET	Separate Effects Test
SFSP	Spent Fuel Storage Pool
SR	Single Rod
TC	Thermocouple

Remark

URL-addresses are valid at the time of writing this document.

1 Introduction

Air ingress during a severe accident in a nuclear reactor might cause an aggravation of damage. Though there is no definite consensus in the scientific community about its probability, this issue has been investigated in the OPSA project of the Euratom Fourth Framework Programme on Nuclear Fission Safety [1] because of its hazards. Firstly, heat release due to oxidation of zirconium by air is 85 % larger than by steam. Secondly, nitrogen forms ZrN. This leads to mechanical degradation of the cladding by formation of scale defects, acceleration the reactions. Details are given in [1].

Meanwhile, off-reactor scenarios on this topic are considered to be more important than reactor scenarios. Therefore, bundle test QUENCH-10, performed on 21 July, 2004 in the QUENCH facility at Forschungszentrum Karlsruhe, was dedicated to this purpose. The related work has been done in the LACOMERA project of the Euratom Fifth Framework Programme on Nuclear Fission Safety [2] and named test QUENCH-L1.

QUENCH-10 was the first test performed in the QUENCH facility that contained an air ingress phase. Up to that time, current experimental knowledge was limited, and the integral severe accident codes were not reliable enough for sufficiently accurate predictions for such experimental conditions, e.g. nitriding of the cladding material during air ingress. So, a number of questions and concerns arose in the experimental and the analytical group likewise about a meaningful test conduct and the integrity of the facility. One of them concerned the hazards of chemical reaction of oxygen with hydrogen during the air ingress phase, the latter produced before and still available in the facility. Other questions referred to consequences of break-away of oxide scale and of nitride formation, reduction of oxide scale during air ingress and temperature escalation during subsequent steam excess. In fact, the test proved to be more benign than supposed before its conduct, but of course this was not known in advance.

Therefore, more decisions had to be taken to define an appropriate test protocol, and hence more analytical work had to be done than normally. It was performed in the successful cooperation of Paul Scherrer Institut, Villigen, Switzerland, and Forschungszentrum Karlsruhe, Germany, that dates back to the preparation of B_4C test QUENCH-07 [3]. It is mainly based on extensive calculations with severe accident codes; but there are also contributions, concerning other than computational aspects, demonstrating that much effort has to be made to allow the conduct of a test that fulfils its desired goals. This report contains the documentation the various aspects of the joint analytical work.

2 Nuclear Scenario

The scenario for this QUENCH test is based on an AEKI proposal. It concerns air ingress during an assumed severe accident in a spent fuel storage pool (SFSP) in the reactor hall of a VVER nuclear power plant [4], as summarised in the following.

The configuration of the respective parts of the nuclear power plant is given in Fig. 2.1. It shows the spent fuel storage tank with racks to store spent fuel elements (blue, centre), and the upper part of the reactor (grey, right). It also shows the cleaning tank (blue, left) which is not a standard component of this system; the pit is normally used to house the transport container of spent fuel. Locks between the components, opened for handling fuel elements, are marked in red.

Due to this configuration, the release of radioactive materials in an SFSP accident bypasses the containment and may cause a danger for the environment. The importance of the accident scenario for safety research is in the possibly large number of fuel assemblies (2 - 3 cores) in the SFSP, involved in the accident, and the limited capabilities to stop such an accident, if it should occur, particularly because there are no dedicated emergency cooling systems for such a case. For clarification, this scenario has nothing to do with the fuel cleaning incident at Paks (Hungary) nuclear power plant of 10 April, 2003 [5].

The assumed accident starts with the loss of operational heat sink due to a break in the cooling loop or loss of components of the decay heat removal system. When the water level falls below the fuel assemblies, air may get access to the hot fuel rods. This may lead to more violent oxidation than with steam and, in case of nearly complete consumption of oxygen (oxygen starvation) to nitriding of the cladding and further degradation in the SFSP. As a consequence, radioactive materials may be released into the environment.

The large water inventory and the low decay heat level result in slow transients: If the accident is not stopped before, it takes many hours, until the water level falls below the fuel assemblies. During this boil-off phase, oxidation is predicted to be heavy in the upper part of the fuel assemblies and small in the lower part because of the low temperature in that region. When air ingress starts, air circulation in the reactor hall cannot guarantee sufficient decay heat removal from all fuel assemblies so that the accident may continue. Based on current knowledge, injection of borated water is considered the only measure to stop further degradation and release from fuel rods, but due to the large volume, filling of the SFSP takes some time. After flooding the SFSP, a small mass flow rate is sufficient to remove the decay heat.

The capabilities of computer codes to simulate such accidents are limited to various aspects, leading to considerable uncertainties in these analyses. Therefore, it was judged that experimental information of a bundle experiment was necessary. Based on calculations with ICARE/CATHARE and FRAP-T6 at AEKI for a number of accident scenarios, AEKI proposed three phases in the QUENCH test, pre-oxidation up to 80 % of the clad thickness, a subsequent air ingress phase without steam at low mass flow rate, and water quench at low injection rate.

It was expected that the bundle test QUENCH-10 would provide new information on the main phenomena of the early phase of SFSP accidents. Special interest was devoted to quenching of nitrided high temperature bundle, for similar tests were never performed before this experiment. The measured data are intended for modelling purposes and as a support to develop an appropriate accident management strategy.

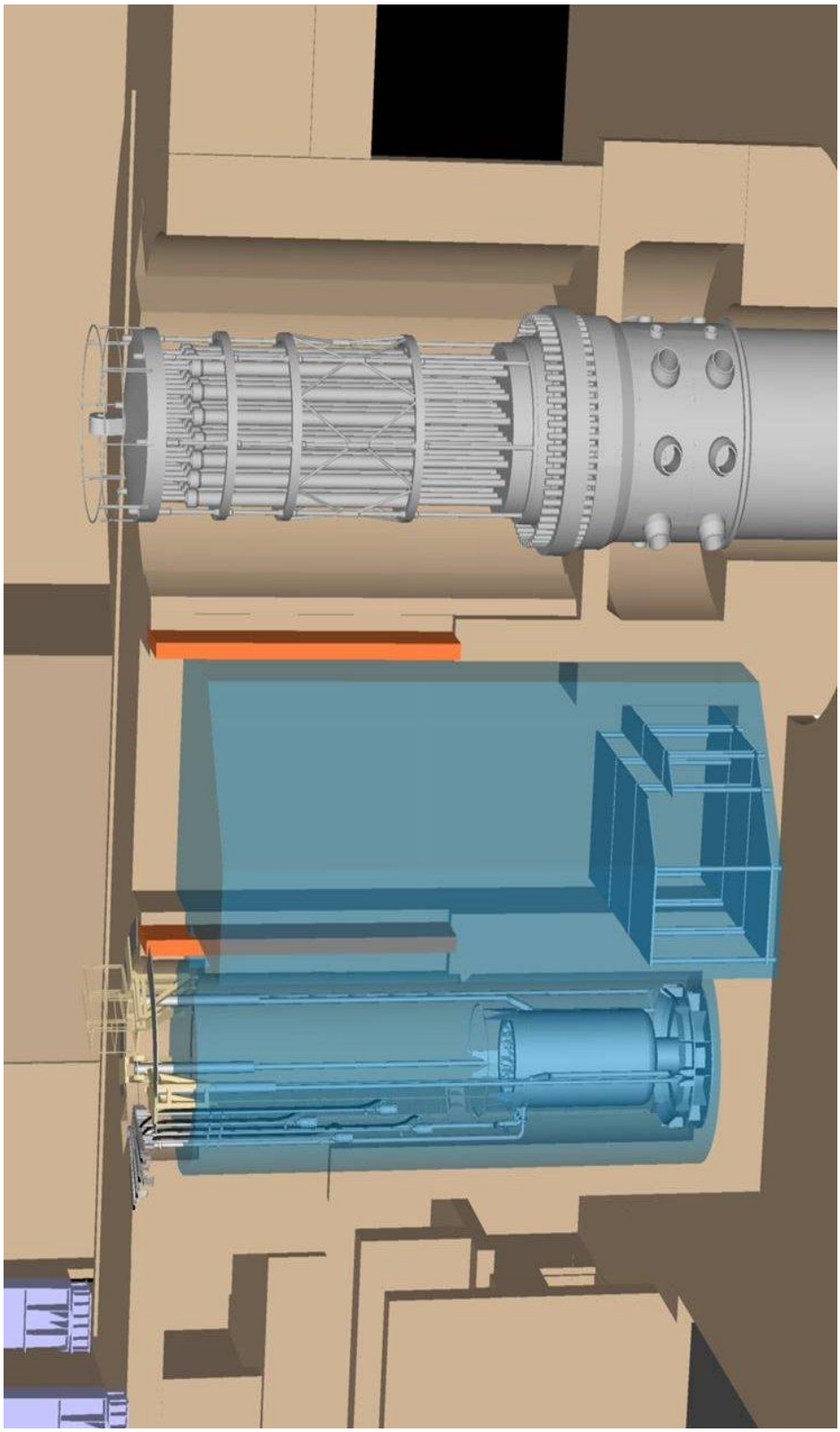

Fig. 2.1: Spent fuel storage pool
(taken from the press conference of the Paks NPP director on 31.08.2004, available on http://www.atomeromu.hu/hirek/hir040901.htm)

3 Experimental Basis

3.1 Quench Facility

In the following a short description of the essential aspects of the QUENCH facility is given. More details are documented in [6]. The QUENCH facility consists of the test section as its main part and a number of external devices (Fig. 3.1). The test section contains a bundle with 21 rods (Fig. 3.2). Their arrangement and their cladding are typical for commercial Western type PWRs. In test QUENCH-10 the central rod is an unheated fuel rod simulator. The other 20 rods are fuel rod simulators with annular ZrO_2 pellets, heated electrically over a length of 1.024 m; the tungsten heaters are connected to a combination of molybdenum and copper electrodes at both ends. Electrical power supply is independent for the eight inner and the twelve outer fuel rod simulators. The four Zircaloy corner rods are intended to flatten the radial temperature profile in the bundle corners; in addition, they are used for instrumentation. In former tests one, meanwhile two of them may be removed during the test to analyze the axial profile of the oxide layer thickness, formed up to that time; the others carry TCs in their centre line. A mixture of steam and argon enters the bundle from the bottom; the fluid, i.e. steam, argon, hydrogen and other products that may be formed or released in the bundle, leaves the bundle at its top to enter the off-gas pipe.

The bundle is contained in a Zircaloy shroud and insulated by ZrO_2 fibre material to achieve an overall flat radial temperature profile in the bundle (Fig. 3.2). This configuration is cooled by counter-current water (upper electrode zone) and argon (heated zone and lower electrode zone) flows within the cooling jackets. The whole set-up is enclosed in a steel containment for safety reasons.

The test section up to and including the outer cooling jacket is equipped with nearly 90 thermocouples at 17 axial locations in the heated section and in both electrode zones. Fluid composition is mainly analyzed by a quadrupole mass spectrometer in the off-gas pipe downstream of the bundle and two aerosol collection systems.

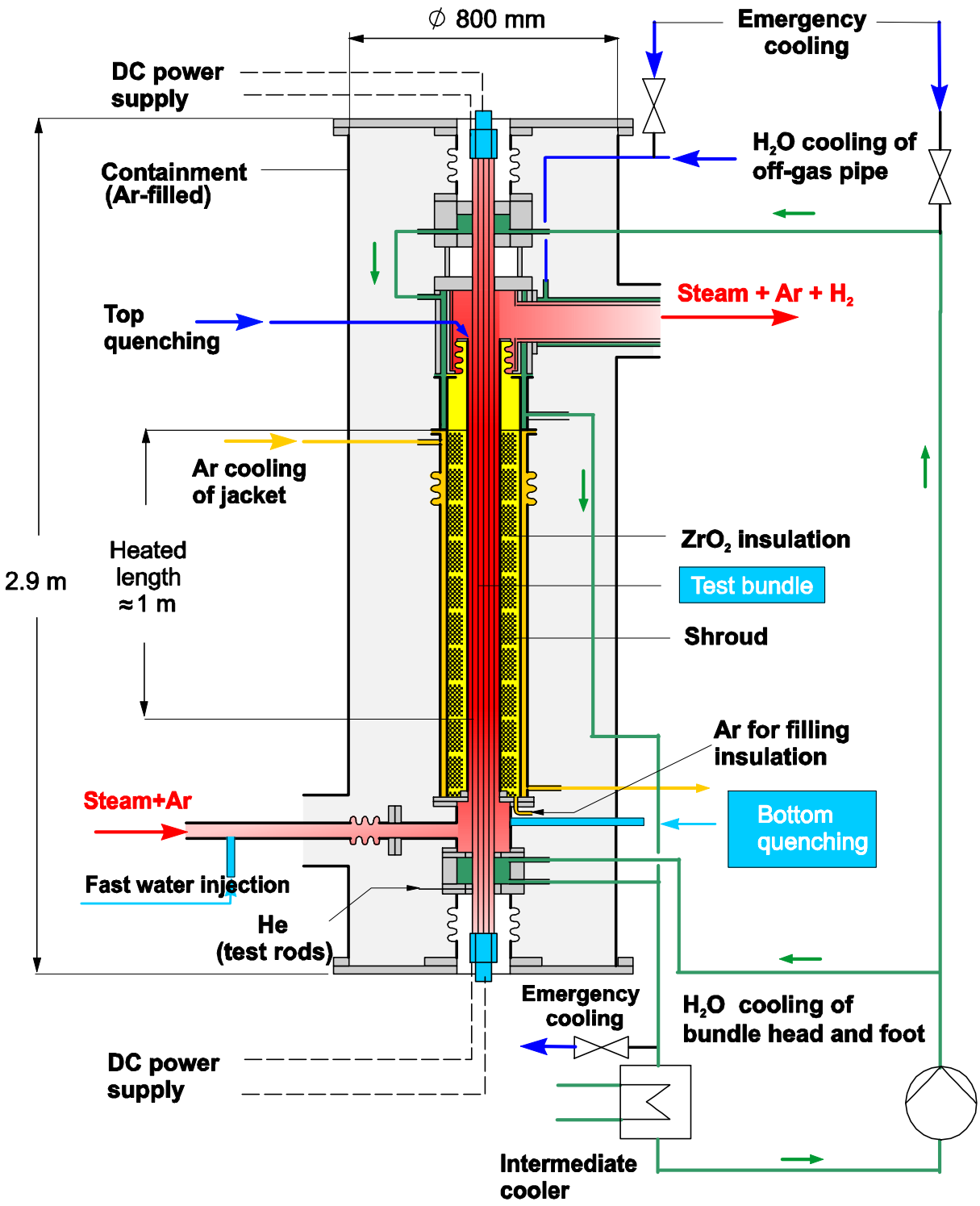

Fig. 3.1: Main flow paths in the QUENCH facility

This figure and the subsequent ones about experimental information are essentially taken from standard QUENCH reports.

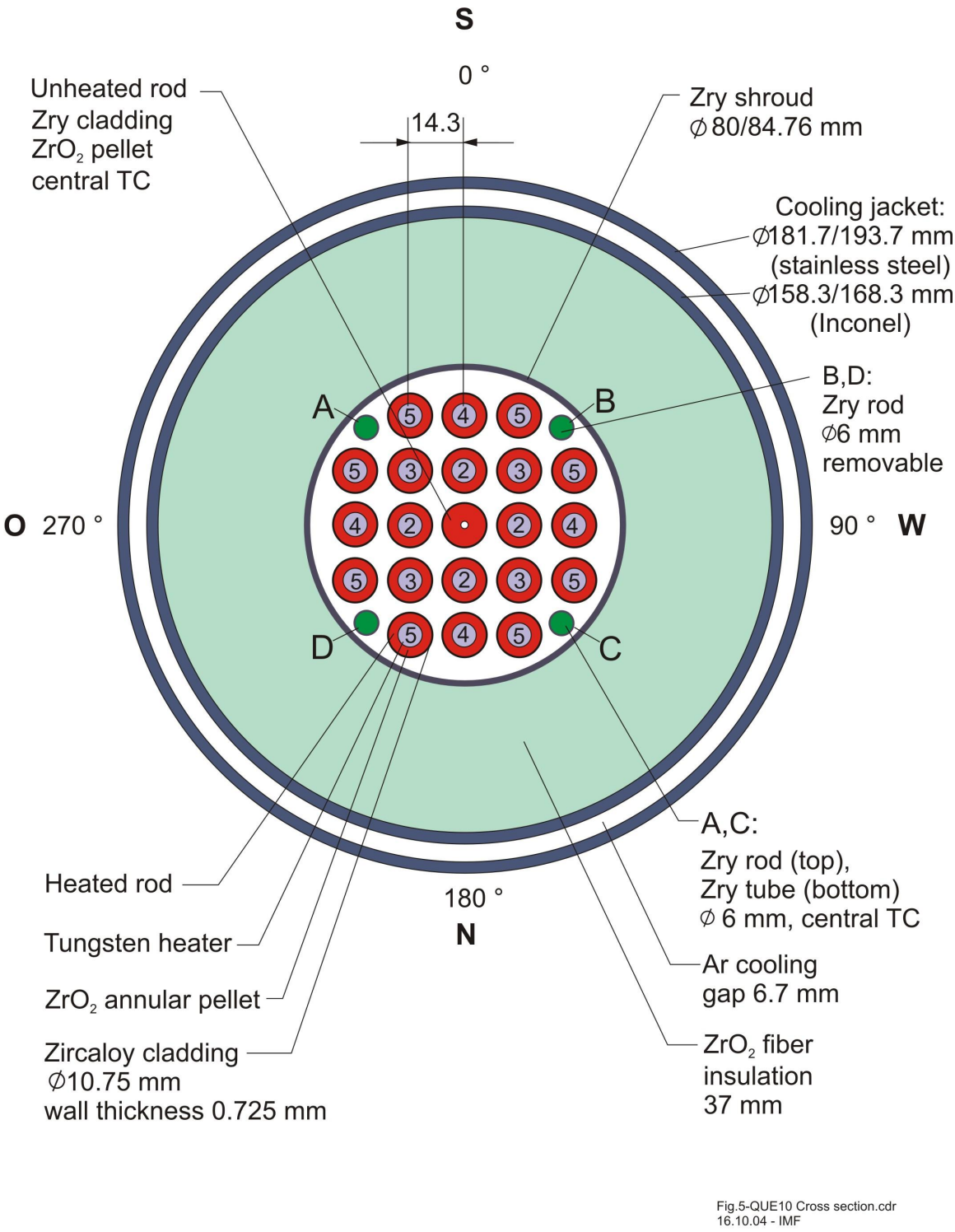

Fig. 3.2: Bundle cross section

The rod numbers indicate different rod types, used e.g. to designate TCs.

3.2 QUENCH Draft Test Protocol

For a number of reasons the SFSP accident scenario, as described above, could not be transferred directly to the QUENCH test. Above all, the QUENCH facility differs substantially from an SFSP. Besides, the 3D flow path in the SFSP is unknown and so are the composition of the atmosphere and the mass flow rate during air ingress as well as the rod lengths and the real configuration of the fuel assemblies in the SFSP at that time. Furthermore, it was thought to be difficult or even impossible to reproduce the long times of the various test phases. In any case, it was assumed that the bundle is essentially intact, when air ingress starts. This was done firstly for practical considerations to simplify the test conduct and the test interpretation and secondly because of the uncertainties about details of the nuclear scenario.

After long discussions to define a draft test protocol, it was agreed to heat the bundle to nearly 900 K (heat-up phase) and perform the various system checks as usual, then to heat the bundle to about 1600 K (first transient), and subsequently to pre-oxidise it up to 600 µm of oxide scale. The air ingress phase should start with a transition from steam flow to 1 g/s air flow without steam. During that phase, 2050 K should be reached, hopefully by oxidation and formation of nitride alone, both exothermal chemical reactions. If these reactions were not sufficient for that aim, electrical power should be increased. Afterwards, the bundle should be quenched with water at a small mass flow rate. During the whole test, an argon flow of 3 g/s is maintained as a carrier gas for measurements with the mass spectrometer. The experimental group suggested that the steam mass flow rate before air ingress was to be determined, the choice being between the standard value of 3 g/s and a value of, say, 1 g/s to be closer to the SFSP scenario and to shift the location of maximum bundle temperature somewhat downwards. A short transition phase with pure argon flow before air ingress was meant to remove the remaining hydrogen inventory in the loop, so that any hazard due to chemical reaction of hydrogen and air, especially in the upper plenum and the off-gas pipe, is excluded.

4 FZK/IRS Calculations

4.1 General

At FZK, SCDAP/RELAP5 (S/R5) mod 3.2 [7] with in-house extensions is used for work on QUENCH tests; at PSI, S/R5 mod 3.2 as a detailed code and MELCOR 1.8.5-RD as an integral code are used for this purpose. In standard S/R5, air and its effects are not modelled, but PSI developed a special version of S/R5 to describe air ingress to some extent, as explained in section 6.1. In MELCOR, the presence of air and air oxidation can be accounted for in the standard version.

Because of these working conditions, FZK pre-test calculations for QUENCH-10 were restricted to the pre-oxidation phase, whereas air ingress and the subsequent phases were dealt at PSI. In this way, one could take advantage of both codes, one code complementing the other. S/R5 input deck and results as well as code changes were delivered to PSI so that PSI specialists could use FZK experience and results as a basis for their own work. Based on extensive calculations in both institutions, the joint effort led to the proposal for the final test protocol.

4.2 Computational Basis

From the very beginning of the project, QUENCH activities have been supported by calculations with S/R5 to define experimental parameters of the QUENCH experiments and to interpret the experimental results after the test. For the calculations presented here, the in-house version of S/R5 mod 3.2 has been used; the new code version, mod 3.3, is still inoperable for applications to QUENCH tests; severe code errors have been reported to the code developers, but user support by the code developer is not any longer available. Among others, the current in-house version contains an improved model for heat transfer in the transition boiling region [8], an adaptation of the CORA heater rod model to the conditions of the QUENCH facility, and the material property data for ZrO_2 instead of those for UO_2 to model the pellets [9]. In contrast to MELCOR, used at PSI for the pre-test calculations, models to describe air flow and oxidation by air are not available.

The various calculations also rely on the experience gained from the calculations done for the previous quench tests. Especially the adjustment of the electrical resistance of the circuit outside the electrical heater rods and the adjustment of the thermal conductivity of the shroud insulation, both based on calculations for test QUENCH-01 [10], were kept.

4.3 Modelling of the QUENCH Facility

The modelling of the QUENCH facility with S/R5 is the same for all tests that are investigated. In the radial direction, the whole facility including the containment is modelled (Fig. 4.1) because the radial heat losses out of the bundle depend ultimately on the ambient room temperature. This modelling is mandatory for all work performed before experimental data are available, and it is desirable for all post-test analyses, because the calculated data are

more detailed than the experimental ones. The model also contains the essential parts of the inlet pipes and the off-gas pipe.

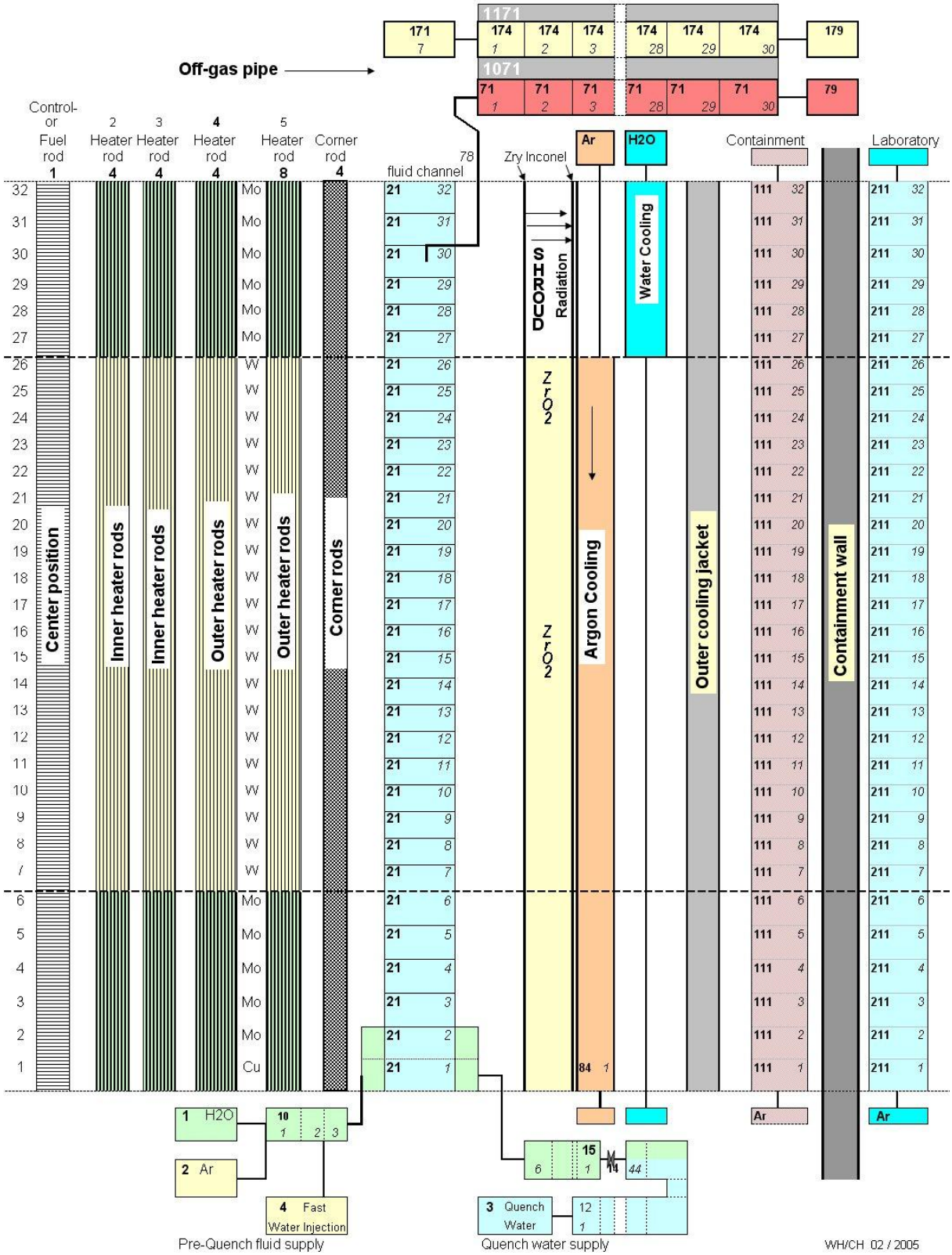

Fig. 4.1: FZK: Modelling of the QUENCH facility with S/R5

The central rod, the two rings of rods to be heated independently, the four Zircaloy corner rods, the shroud with its insulation, the inner and outer cooling jacket, and the containment are modelled as SCDAP components. The ZrO_2 fibre insulation is modelled to end at the upper end of the heated zone. With this exception, all structures must be modelled to have the same length because of limitations in the code. Therefore, the upper and lower head cannot be modelled in all details.

The region of the heated part is axially modelled with 20 5 cm long mesh cells. In the lower and upper electrode zones 0.45 and 0.6 m, respectively, of the test section are considered, each by six mesh cells (32f model). For calculations of the quench phase, these mesh lengths are consistent with [11]. In that reference, a maximum of 0.07 m (3") is suggested; in case of much larger meshes, averaging of temperatures and heat fluxes smear the very pronounced temperature drop (quenching) leading to reduced cool-down rates, but also for former test phases, the results may be improved. Details about the S/R5 model are essentially given in [12]. The inlet pipe for steam and argon is modelled with six 15 cm long meshes between the valve that is closed at quench initiation and the inlet plenum; the quench water pipe is modelled with 21 15 cm long meshes between the pump and the inlet plenum.

4.4 FZK/IRS Calculations

Calculations have been done with the standard fluid composition of 3 g/s steam and argon each, the inlet temperature being 600 K. Initial conditions are set as in QUENCH-09. The electrical power for the first transient is adjusted to give a temperature rise smaller than that of QUENCH-05, but faster than in QUENCH-09 and to reach a maximum temperature of about 1600 K for pre-oxidation. Later in the pre-oxidation phase, electrical power is increased to maintain a more or less constant hydrogen production rate. We proposed this procedure for QUENCH-01 [10], and it is used since then. For QUENCH-10, a value of about 5 mg/s seems reasonable. In this way, maximum bundle temperature increases with time, but pre-oxidation is by far faster than when it is performed at constant temperature. Results for the variation of electrical power are given in Fig. 4.2 and Fig. 4.3. They also indicate the amount of work to derive the test protocol and the sensitivity of the response of the facility, when electrical power is changed.

Time dependent results for the final calculation, proposed for the test protocol, are given in Fig. 4.4. According to the calculation, oxide scale eventually increases nearly linearly with 0.05 µm/s near the upper end of the heated zone so that the envisaged maximum oxide scale of 600 µm is reached at 11070 s, corresponding to more than 9200 s of pre-oxidation. The maximum bundle temperature at that time is 1713 K. It increases to 1745 K at the end of the calculation, i.e. to a value shortly below a temperature escalation starts, when the oxide scale is still thin. The experimental group was rather sure that the hazard of a premature temperature escalation would be small at the end of the first transient, when electrical power must be reduced, because they had gained enough experience from previous QUENCH tests. It would also be small for small oxide scales, because the temperature would not be exceptionally high. Finally, it would remain small later on, when temperature increased, because oxide scale would be rather large at that time. Axial profiles at times when maximum

oxide scale is 100, 200, 300, … µm (Fig. 4.5) show that temperature profile does not change much during the whole time, and for all variables, shown in that figure, maxima are near the end of the heated zone.

To prepare calculations for a steam mass flow rate of 1 g/s, requested by the experimental group, pre-test calculations for QUENCH-07 [3] were reviewed. They predict for such a mass flow rate that the facility reacts rather sensitively, when electrical power is changed as it is necessary during the test. This sensitivity also entails laborious pre-test calculations. The calculations for QUENCH-10 for standard fluid composition show that not more than about 0.5 g/s steam are consumed for oxidation so that steam starvation that might be expected in the nuclear scenario should not occur and the shift of maximum bundle temperature towards the bundle centre and hence the shift of the oxidation profile is expected to be small, about 10 cm only. Due to the steep temperature decrease at the end of the heated zone, this would not give much more information downstream of the temperature maximum, as it was a second aim for this proposal. Besides, it was expected [13] that the morphology of the oxide scale would not differ much in these two cases. Therefore, it was decided after intensive internal discussions to use standard fluid composition up to air ingress.

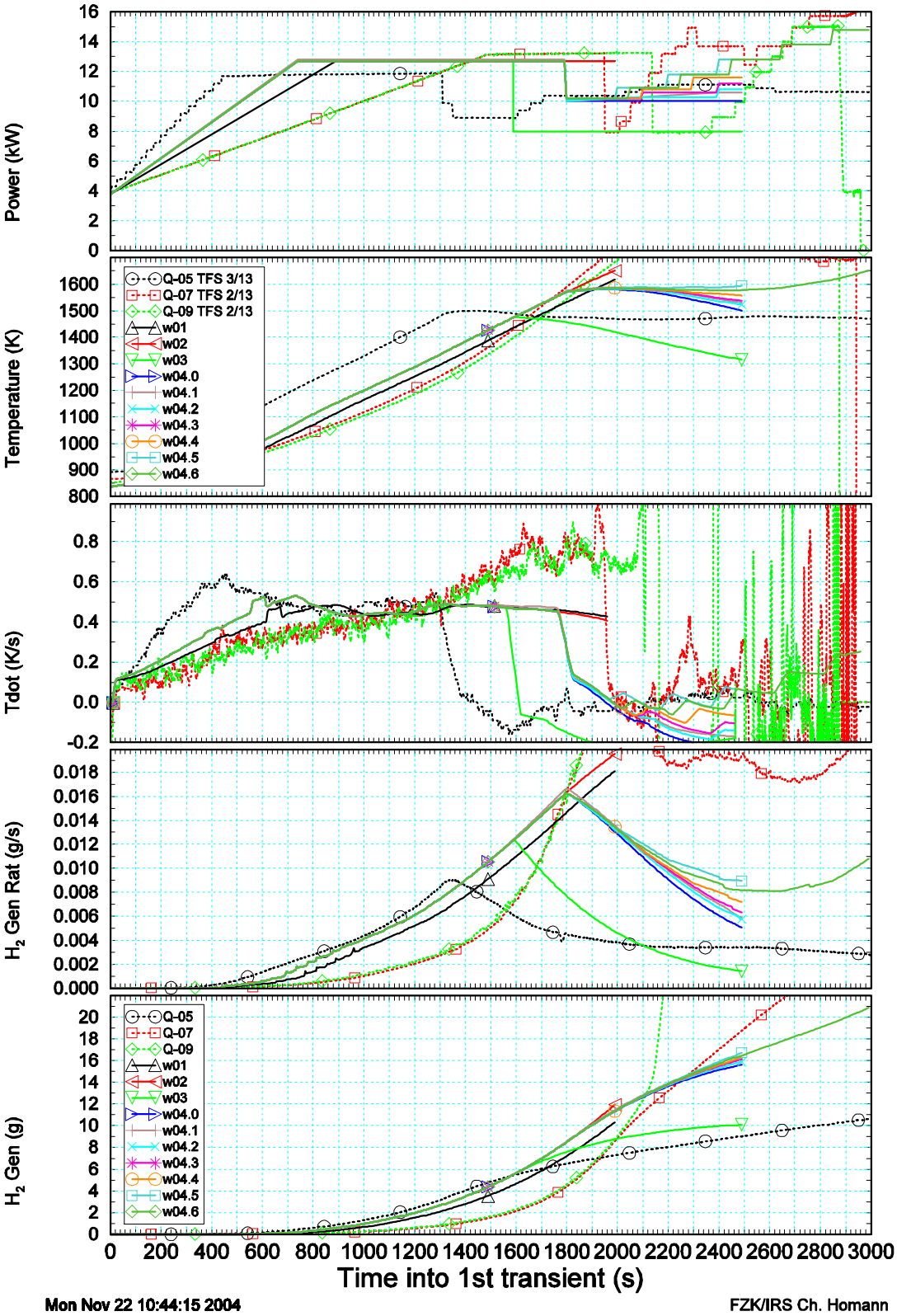

Fig. 4.2: FZK: Survey of pre-test calculations (part 1)

The figure shows from top to bottom electrical power input, clad surface temperatures of inner heated rods at elevation 0.925 m together with experimental values for QUENCH-05, -07, and -09, temperature derivatives with respect to time, hydrogen production rate, and hydrogen production for various computational runs. In this and the following plots legends also refer to the graphs above the respective legend.

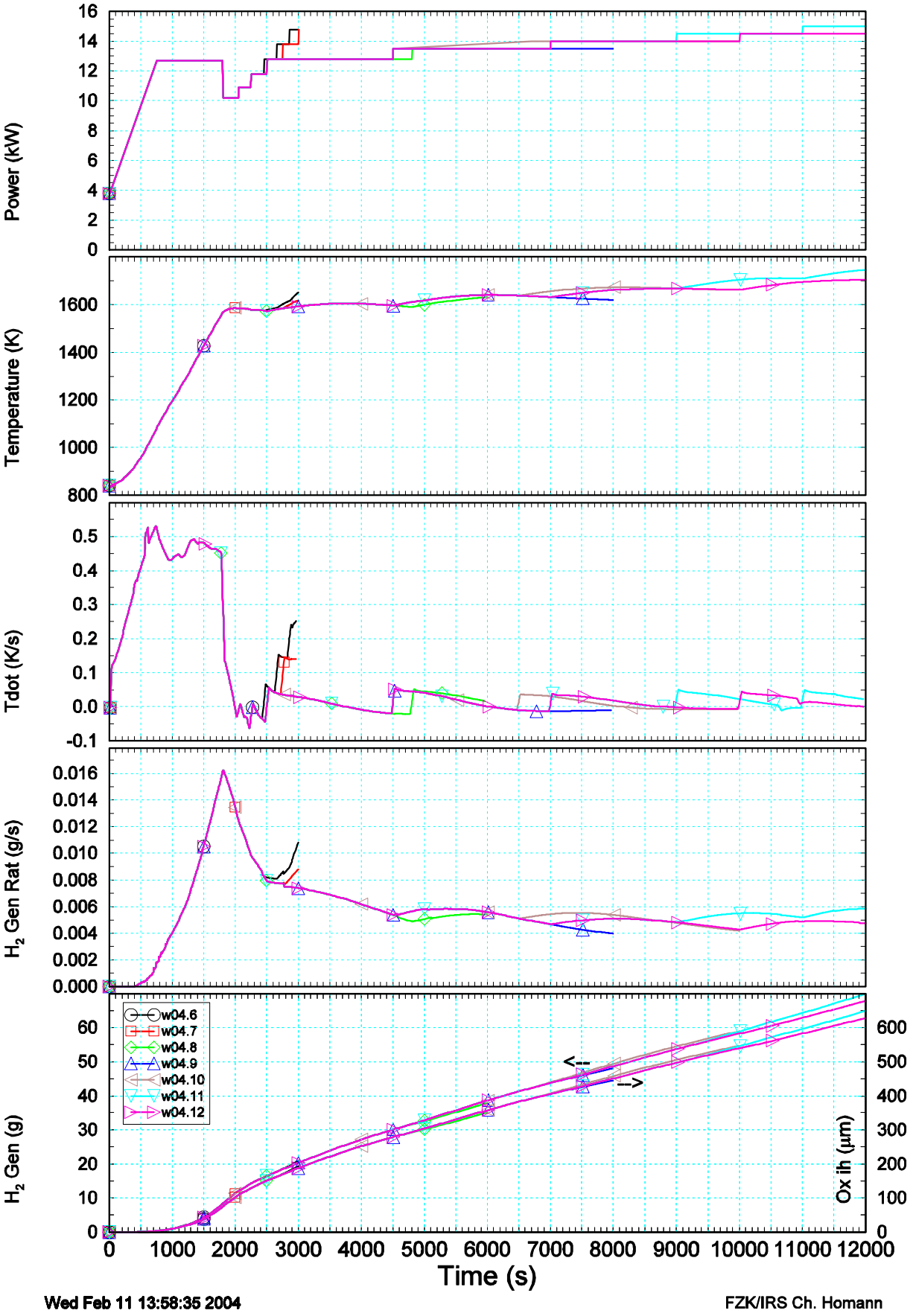

Fig. 4.3: FZK: Survey of pre-test calculations (part 2)

The layout of this figure is as for Fig. 4.2. The arrows indicate the respective scales.

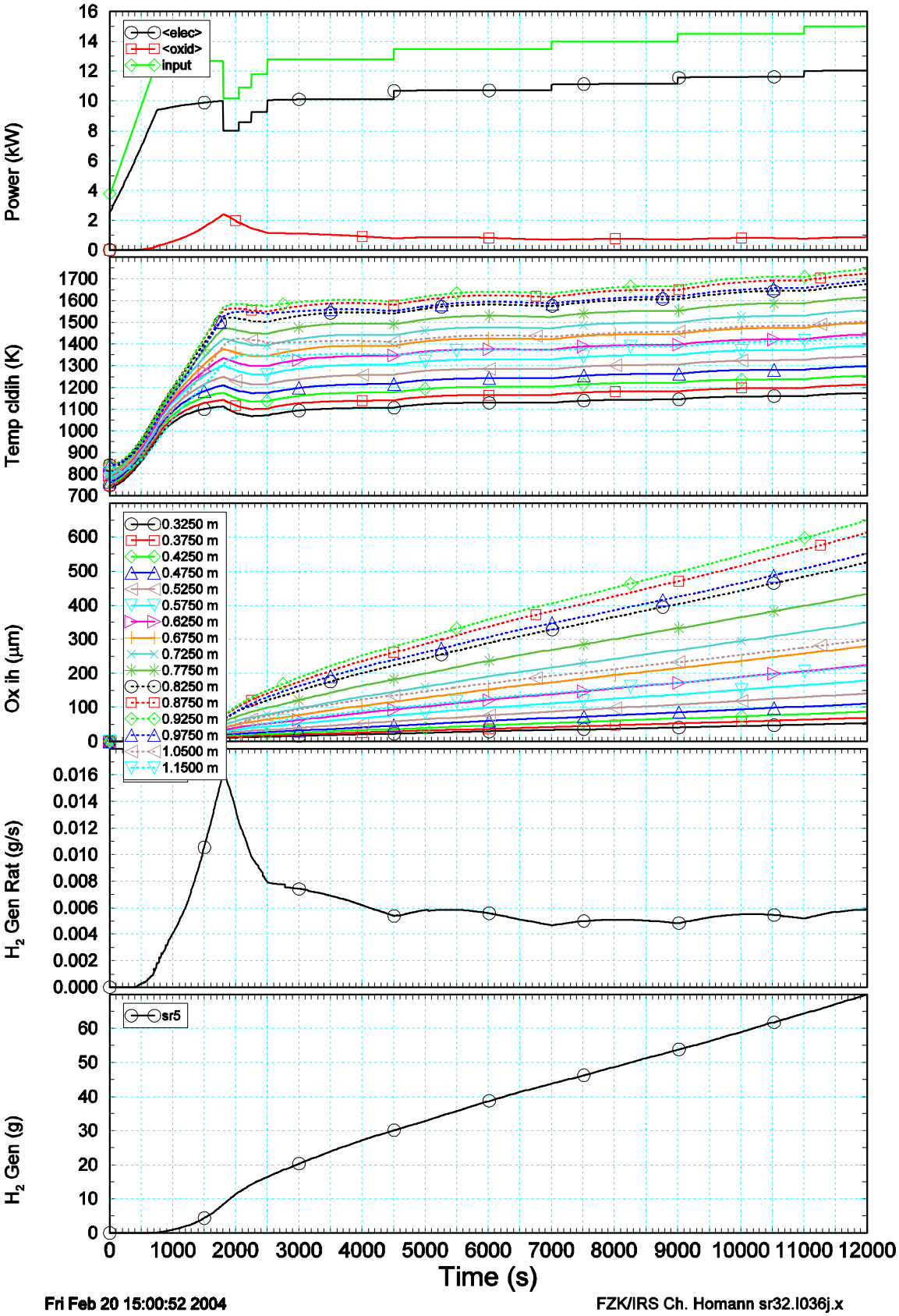

Fig. 4.4: FZK: Time dependent results of final pre-test calculation

The figure shows from top to bottom electrical power input, clad surface temperatures and oxide scale of inner heated rods at elevation 0.925 m, bundle hydrogen production rate, and hydrogen production.

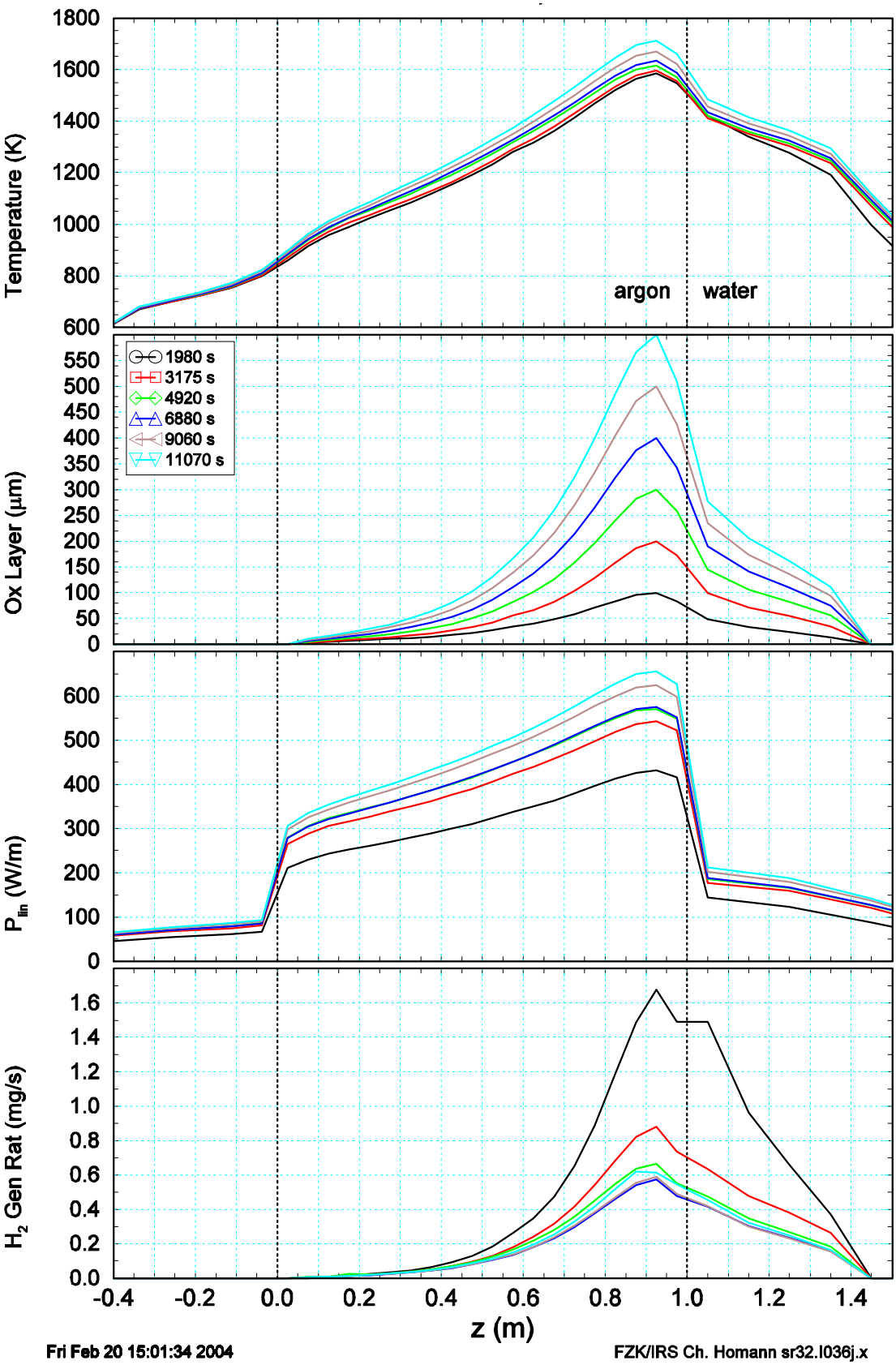

Fig. 4.5: FZK: Axial profiles for selected variables for final pre-test calculation

The figure shows from top to bottom clad surface temperatures, oxide scale, and linear rod power of inner heated rods, and hydrogen production rate in the bundle at various times.

5 Other Analytical Work at FZK/IRS

5.1 Oxide Scale in S/R5

In pre-test calculations for previous tests it has been remarked that for heavy oxidation the oxide scale, S/R5 output variable oxdeo, increases steadily to more than 700 µm, then jumps to a value of more than 1 mm and remains constant irrespective of temperature. A similar error occurs for the outside radius of the cladding, rco; but the coordinate of the inner oxide scale boundary and the oxide scale sum up to the outside radius of the cladding, as it should be. For these calculations, the standard correlations for oxidation are used, i.e. Cathcart for low and Urbanic-Heidrick correlation for high temperatures. Since this error normally had no impact for the preparation of tests, it was not investigated further before the preparation of QUENCH-10.

Comparison between post-test calculations of the various tests and measured data suggest that variable oxdeo really refers to oxide thickness and not to the thickness of consumed metal, the respective ratio being known as Pilling-Bedworth (PB) ratio. Hand calculations also show that the step, mentioned above for pre-test calculations for QUENCH-07, is 1.46 and hence different from PB ratio of somewhat more than 1.5 for ZrO_2 and also different from the ratio of molecular weights of ZrO_2 and Zr (1.35).

For the preparation of QUENCH-10, however, some care should be spent on this item. At FZK/IMF, oxidation of the central rod over its whole length has been calculated with SVECHA/Q [14] using the temperature history, calculated with S/R5, as input. The central rod was chosen, because it is unheated and any problem that might have to do with heating is circumvented. To evaluate the SVECHA results, data were extracted for axial levels 675, 925, and 1250 mm. For time reasons, no more work could be spent on this issue.

In addition, separate effects tests (SET) with rod specimen were performed in the QUENCH-SR rig to investigate pre-oxidation [14]. In these tests, the temperature histories at axial elevations 475 mm, 675 mm, and 925 mm, calculated with S/R5, were used. From the photos of bundle cuts after pre-oxidation, we derived oxide scales. The complete set of data for calculations and SETs is given in Tab. 5.1 together with characteristic temperatures T_{ch} at the respective level, being approximately the same for both times.

Tab. 5.1: Calculated and measured oxide scales at 8000 and 11000 s

z [mm]	T_{ch} [K]	Oxide scale [µm]				
		S/R5	SVECHA	S/R5	SVECHA	SET
		8000 s		11000 s		
475	1250			87		20
675	1500	176	161	234	240	277
925	1700	419	594	551	859	~ 1000
1250	1350	124	125	161	184	

Fig. 5.1 shows the hydrogen production for the whole central rod and at its hottest position, at 925 mm, as calculated with both codes. Deviations from one another may come from different oxidation models: In SVECHA, diffusion coefficients for oxygen, based on the experimental work of Pawel and Cathcart and of Leistikow and Schanz, are used to calculate oxidation for this temperature range, whereas S/R5 relies on Leistikow and Schanz correlation directly. Besides, threshold temperature, where oxidation is modelled to start, is different. Overall differences can be assessed from the cumulated hydrogen production. For the purpose of the test preparation, these differences are considered to be acceptable.

Evaluation of SVECHA results for the thickness of β-Zry, α-Zr(O), and oxide scale was done at axial elevations 675 mm, 925 mm, and 1250 mm and compared to S/R5 results. As an example of time development, results for axial elevation 0.925 m are shown in Fig. 5.2. In S/R5 not all data were available for the central rod; in this case results for the central heated rods are presented. At elevation 0.925 m, it is only the oxide layer that shows increasing differences between the two programmes; the scale ratio approaches a value of about 1.6 for later times of pre-oxidation. Oxide scales at elevations 0.675 and 1.25 m agree much better. At elevation 0.675 m, the extension of β-Zry is predicted to be larger by SVECHA. The same is true for the extension of α-Zr(O) at elevation 1.25 m.

Axial plots of the relevant variables at 8000 s, as calculated with S/R5 and SVECHA (Fig. 5.3), and, together with oxide scales from the SETs, at 11000 s (Fig. 5.4) give an overall picture. These two figures suggest that oxide scales, calculated with S/R5, give larger differences with SVECHA and SETs only for large scales, whereas the β-Zry and α-Zr(O) layers agree quite well.

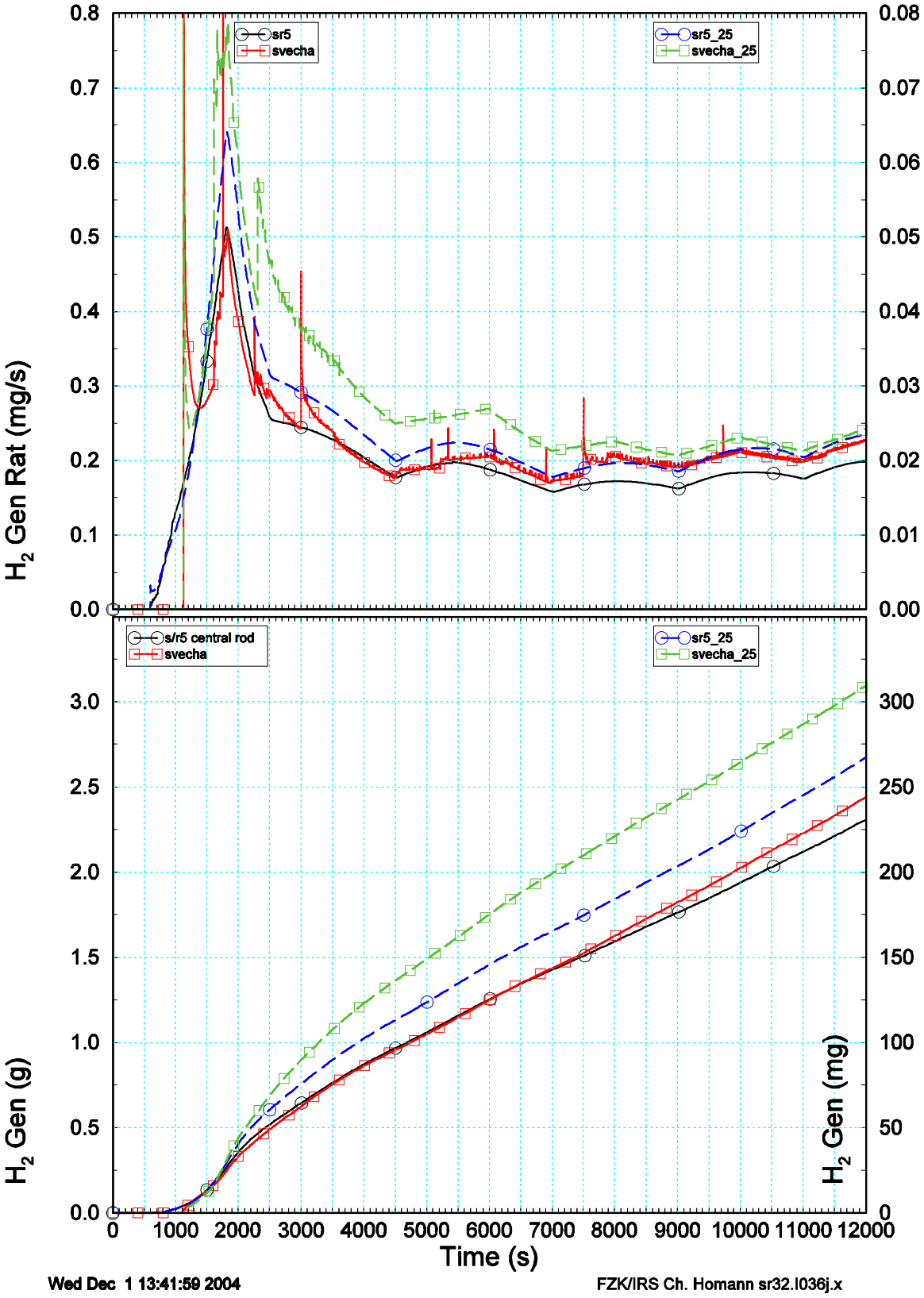

Fig. 5.1: FZK: Hydrogen generation in central rod, calculated with S/R5 and SVECHA

The figure shows hydrogen generation rate (top) and cumulated hydrogen generation (bottom) for the whole central rod (left scale) and at elevation 0.925 m (right scale, label _25), calculated with S/R5 and SVECHA, as a function of time.

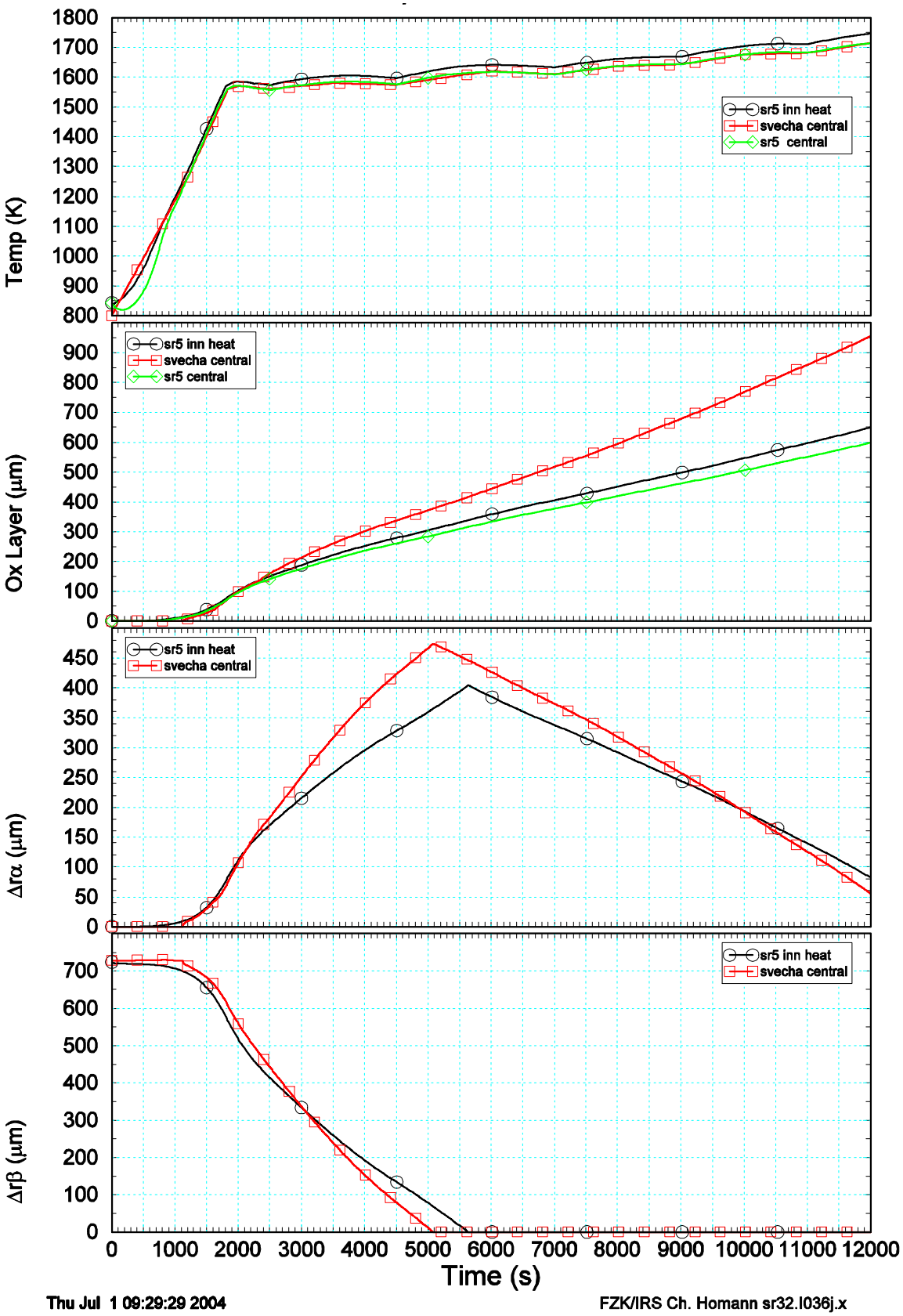

Fig. 5.2 FZK: Central rod results, calculated with S/R5 and SVECHA

The figure shows from top to bottom outer clad temperature, oxide scale, thickness of α-Zr(O) and β-Zry at axial elevation 0.925 m as a function of time.

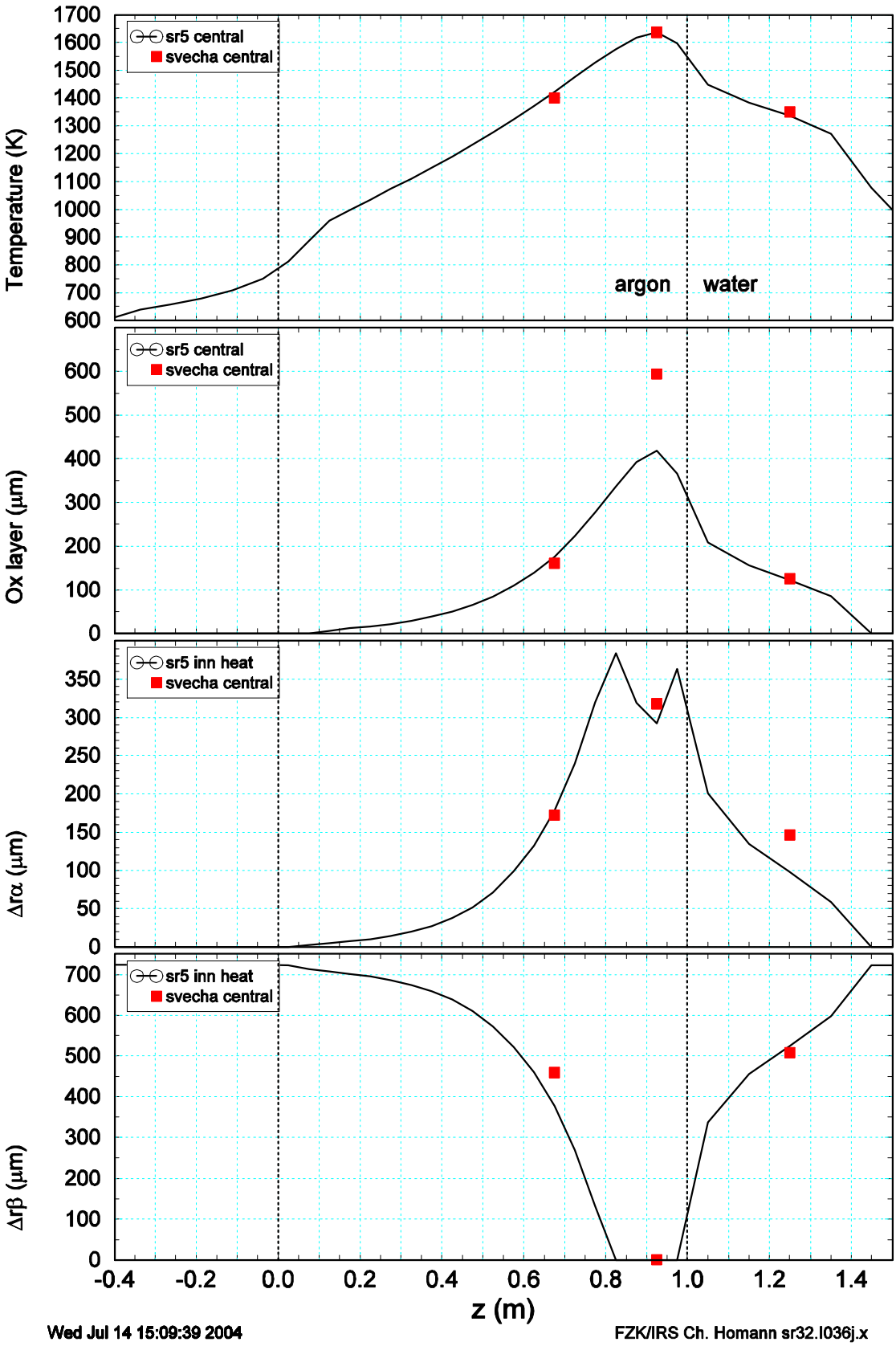

Fig. 5.3: FZK: Axial profiles of clad data at 8000 s

The figure shows from top to bottom axial profiles of outer clad temperature, oxide scale, thickness of α-Zr(O) and β-Zry, calculated with S/R5 and SVECHA.

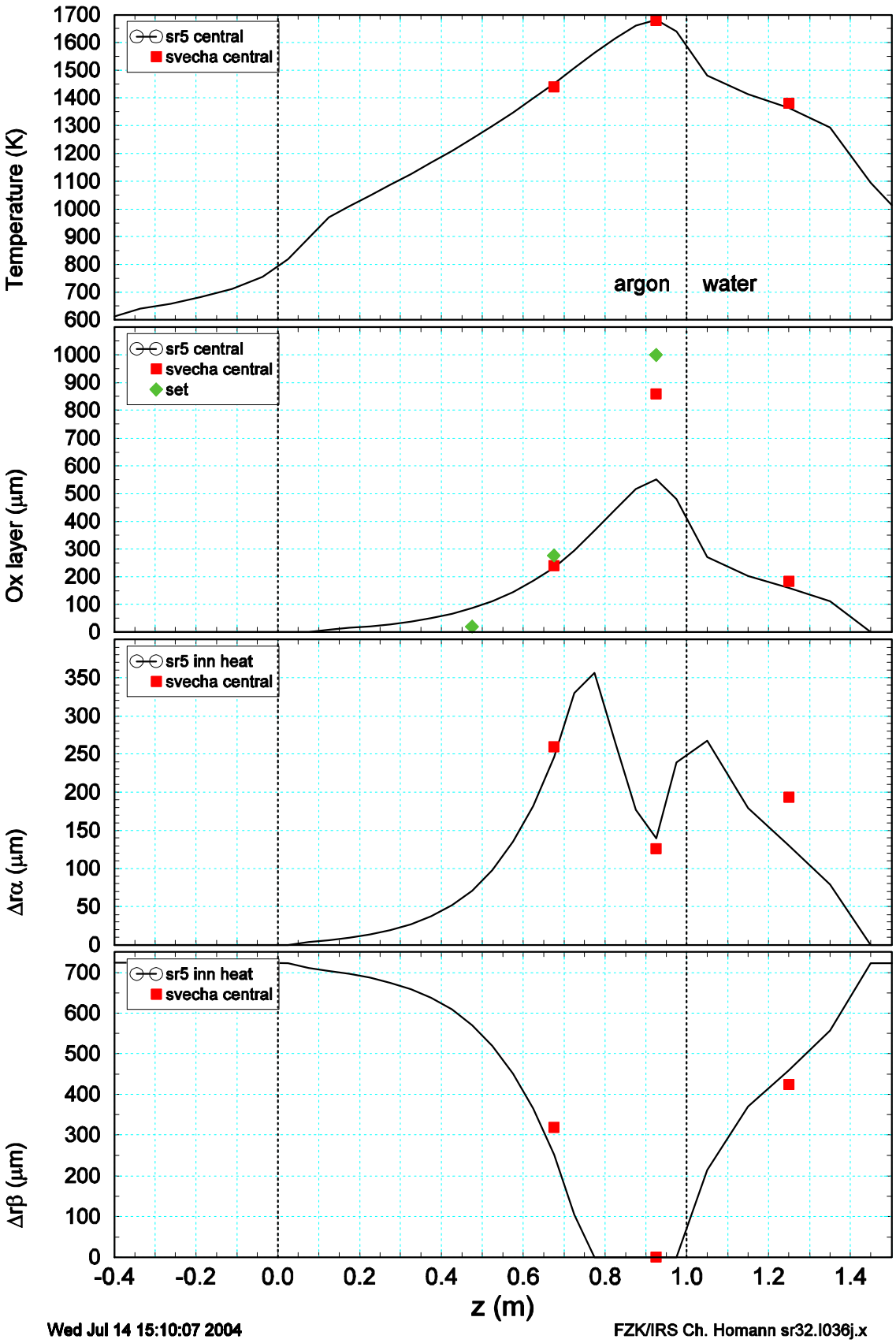

Fig. 5.4: FZK: Axial profiles of clad data at 11000 s

The layout is the same as for Fig. 5.3.

5.2 Contributions to Experimental Issues

Due to the long pre-oxidation phase, TCs in the hot zone that are in direct contact with the fluid are expected to fail before air ingress. Since these high temperature TCs are very expensive, we suggested reducing their number, but taking care that information of the bundle status during pre-oxidation is still sufficient. As a consequence of this reduction, the instrumentation is restricted in comparison to some other QUENCH tests, especially those without pre-oxidation. It is emphasized that for the present test the number of TCs in the facility is nevertheless still rather large to derive quantitative information. Operators must be aware of this shortcoming and rely on protected bundle and shroud TCs and keep in mind a certain delay due to thermal inertia and a difference to maximum bundle temperature because of the radial temperature profile and perhaps also of axial temperature profile, if all TCs at that axial level should fail. From the outcome of the PSI work for air ingress phase, discussed later, it was suggested to introduce high temperature TCs in the centre of the heated zone.

Since TC instrumentation in the bundle and hence quantitative information is reduced during air ingress in comparison to other QUENCH tests, it was also suggested to withdraw two corner rods during the test, one shortly before the start and one at about the end of air ingress. For the second corner rod, the clearance of the spacer grids should be increased so that especially the second corner rod can be withdrawn in spite of the expected thick oxide and nitride scale and of the possible bending of the corner rod. The experience that the second corner rod broke at axial elevation 885 mm, underlines the importance of this item.

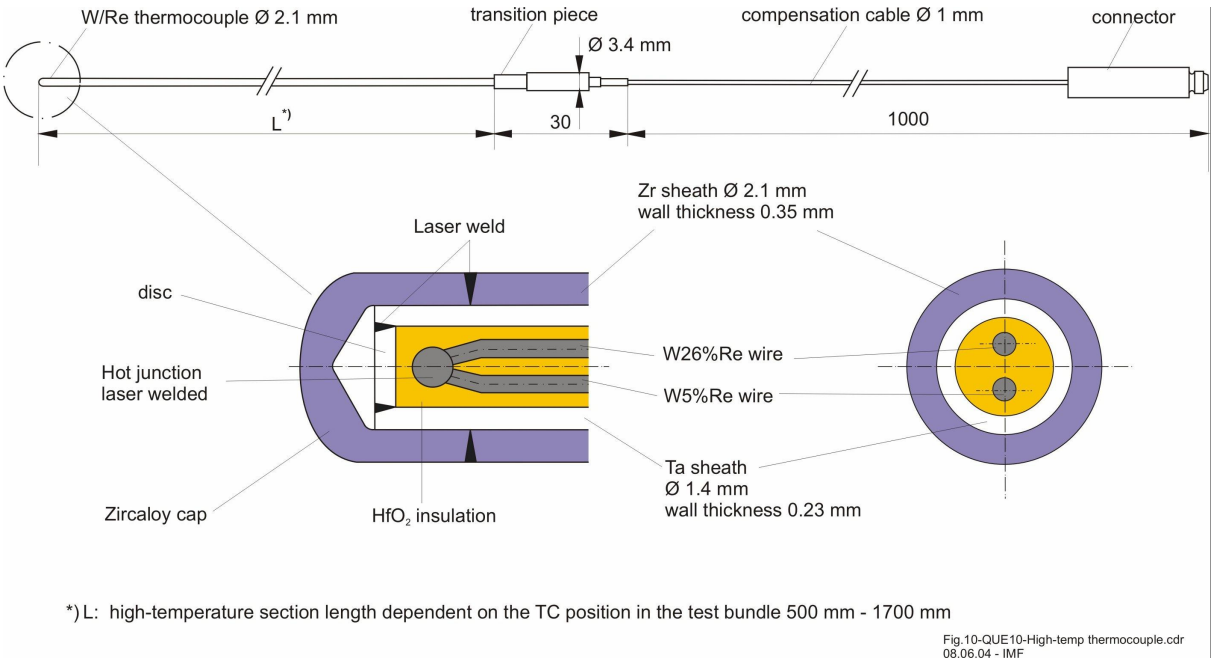

Fig. 5.5: Current design for high temperature TCs

It was further suggested to pre-oxidize the inner surface of the Zr sheath of high temperature TCs. In this way, the Ta sheath (Fig. 5.5) becomes superfluous and some amount of space can be saved. In this way, disturbance of the fluid flow is reduced. This is not only a general improvement, but it is of major importance for two-phase flow conditions, where TCs are obstacles in the path of droplets. Secondly, oxidation of the inner surface of the Zr sheath by reducing HfO_2, as it occurs in present design and causes TC failure, is of less importance

due to the contact of ZrO_2 and HfO_2, and TC failure may be postponed. As a further advantage, high temperature TCs become more flexible and hence less vulnerable to destruction during handling. For time reasons, this proposal could not be realized in this test, but preparation work has begun for future applications.

After shroud failure, the outer shroud surface contributes to oxidation and, in this way, complicates interpretation of experimental data. To avoid this side effect, it was suggested to maintain slight overpressure in the region between shroud and inner cooling jacket by a small argon flow after shroud failure. This additional argon flow must be taken into account to evaluate MS data.

The proposal when to end the pre-oxidation phase will be discussed in section 7, because it also relies on PSI calculations with MELCOR and S/R5. As in previous tests, measured maximum temperature and its time derivative should be compared with predicted ones during sensitive test phases to optimize the test conduct and to detect deviations from the intended test protocol that might jeopardise an appropriate test conduct and miss its aims as early as possible.

6 PSI Contributions

6.1 Introduction

Planning calculations were performed at PSI using a modified version of S/R5 mod3.2hx to simulate the effect of oxidation in air, and MELCOR 1.8.5-RD which accommodates as standard features the presence of air and air oxidation, as well as a model for reflood quench which was benchmarked during the course of the OECD International Standard Problem ISP-45 [6]. The starting point for the present calculations are the S/R5 and MELCOR input models used in previous analyses of QUENCH experiments, modified according to the provisional time-dependent boundary conditions for electrical heating, inlet flow and composition [16].

The MELCOR hydraulic model comprises one channel for the bundle, with four axial nodes over the 1 m of the heated section. However, ten axial nodes are used to model the bundle components (the COR input) within the heated section (numbered 06-15 in subsequent plots). The outer surface of the inner cooling jacket is modelled as a boundary condition rather than as a hydraulic system. Supplementary coding is supplied by the MELCOR developers to enable modelling of the electrical heaters.

The S/R5 hydraulic model also includes one channel for the bundle, with four SCDAP components inside the shroud, these representing the central unheated rod, the first ring of eight simulator rods, the second ring of twelve simulator rods, and finally the four corner rods. Sixteen axial nodes are used, with three each for the upper and lower electrode regions, and the remaining ten for the tungsten heater zone (numbered 04 - 13 in subsequent plots). The SCDAP model also includes components for the shroud, inner and outer cooling jacket, and containment, with corresponding hydraulic modelling of the argon cooling, of the water cooling, and of the containment atmosphere. The level of modelling is therefore more detailed than in the MELCOR case, in particular concerning explicit representation of the corner rods.

The electrical heating transient was specified to provide an initial heat-up to about 1600 K, followed by a plateau phase lasting several thousand seconds while the cladding progressively oxidises to a prescribed extent (maximum oxide scale in the bundle 600 µm). The inlet flow would then be changed from 3 g/s steam plus 3 g/s argon to 1 g/s air plus 3 g/s argon. Reflood quench or cool-down in an inert gas would be initiated at a maximum measured temperature of 2073 K. The power history were based on those supplied by FZK; essentially power is raised stepwise to a level of about 14 kW in such a way as to minimise the possibility of an excursion taking place. Typical power and fluid flow histories are given in Tab. 6.1 and Tab. 6.2.

The MELCOR code includes as a standard feature specification of all the constituent gases used in QUENCH experiments, and furnishes separate models for oxidation by steam and oxygen. The S/R5 code does not provide a means of modelling air (or oxygen) as an oxidizing gas. For present purposes a modification was made to the Zircaloy-steam oxidation model to replicate the kinetics and heat of reaction (per mole) of oxidation by oxygen. This version is used for the air ingress period, with the steam flow defined to give the same num-

ber of atoms of oxygen as with the prescribed flow of air. It is noted that the gas composition and molar flow are not preserved. The argon flow was increased to simulate cooling and transport properties of the 0.8 g/s nitrogen that would be present in the air. Neither MELCOR nor S/R5 has models for nitride formation. It is noted that similar kinetics were used by JRC Ispra to simulate successfully the CODEX-AIT1 air ingress experiment [15] in the EC 4th Framework OPSA project [1]. Details of the modelling are given in Tab. 6.3. The authors are aware that material property data of air instead of steam are necessary for better predictions, but program changes could not be done in time.

Tab. 6.1: Typical power histories for S/R5 calculations

Base case – no cooling		**'Air' ingress + Water quench, with power reduction**	
Time, s	Power, W	Time, s	Power, W
0	3800	0	3800
10	3800	10	3800
750	12700	750	12700
1800	12700	1800	12700
1805	10200	1805	10200
2050	10200	2050	10200
2055	10900	2055	10900
2250	10900	2250	10900
2255	11800	2255	11800
2500	11800	2500	11800
2505	12800	2505	12800
4505	12800	4505	12800
4510	13500	4510	13500
7005	13500	7005	13500
7010	14000	7010	14000
8250 (calculated time to 600 µm oxide)	14000	8250	14000
		8280	7000
		12400	7000
		12415	3900
		12600	3900
		12615	0
14000	14000	14000	0

Note: In the constant power cases, the power is continued at 14 kW.

Tab. 6.2: Typical fluid flow histories for S/R5 calculations

Base case – no cooling			**'Air' ingress + Water quench**				
Time, s	Ar, g/s	Steam, g/s	Time, s	Ar, g/s	Steam, g/s	Air, g/s	Water, g/s
0	3	3	0	3	3	0	0
			10750	3	3	0	0
			10780	3 [1])	0	1 [2])	0
			12400	3 [1])	0	1 [2])	0
			12400.1	0.	0	0	800
			12405	0	0	0	800
			12405.1	0	0	0	50
14000	3	3	14000	0	0	0	50

[1]) 1.3 g/s added to this to simulate mass flow of nitrogen in air
[2]) Simulated by 0.225 g/s steam

Note: The histories for MELCOR are very similar, being basically time-shifted after the pre-oxidation is deemed to be complete; also the 'air' is input as air, rather than being simulated by steam, so also no additional argon flow is imposed during the air period.

Tab. 6.3: Details of oxidation modelling

Steam	$Zr + 2\ H_2O = ZrO_2 + 2\ H_2$	Urbanic-Heidrick
Δh	5.797×10^6 J/kg$_{Zr}$	
K(T)	29.6 exp (-16820/T)	T < 1853 K
K(T)	87.9 exp (-16610/T)	T > 1873 K
Air	$Zr + O_2 + N_2 = ZrO_2 + N_2$	Benjamin et al., NUREG/CR-0649
Δh	1.2065×10^7 J/kg$_{Zr}$	
K(T)	50.4 exp (-14630/T)	= 12.7 x K_{steam} at 1500 K

Diffusion limits apply

dW/dt	(M k_c P_{ox}) / (n R T_f)
M	molecular weight
k_c	mass transfer coefficient
P_{ox}	partial pressure of oxidant
n	moles of oxidant consumed per unit mass of Zr
R	gas constant
T_f	gas film temperature (T_{Zr} + T_{gas}) / 2

Notes: 1) Parabolic kinetics - units of K are kg$_{Zr}^2$ / m^4 s^2.
2) Model found to give fair agreement with CODEX AIT

6.2 Pre-oxidation and Air Ingress

Calculated inner ring cladding temperatures for the provisional scenario using S/R5 and MELCOR are compared in Fig. 6.1. Both codes calculated the initial temperature ramp and plateau according to the planned evolution. The prescribed oxide thickness was achieved at about 10000 s with MELCOR and somewhat earlier, at about 8250 s, with S/R5, see Fig. 6.2 (plotted as thickness of metal reacted, 0.67 times the oxide thickness). This is in line with the higher temperatures predicted by S/R5 at the top of the bundle; the axial temperature gradient was also steeper according to S/R5, so the temperatures at the bottom were cooler. The oxide thickness stopping criterion was applied to the inner heated ring, whereas the corner rods, which can be pulled from the bundle at chosen times, are cooler and this results in lower oxide thicknesses. The figure indicates the difference that might be expected, and which should be considered in subsequent analysis.

Following the switch from steam to air MELCOR and S/R5 calculations showed a rapid temperature escalation due to the combined effects of increased oxidation kinetics and reduced convective heat transfer, which resulted in a fairly short period before the temperature criterion for quench initiation. S/R5 calculations show that much of the increased heating rate is due to the reduced heat transfer; compare Fig. 6.3 and Fig. 6.4, so that isolating the effect of air oxidation itself would be difficult (the difference is most notable at the bottom of the bundle, which is of not so much of interest regarding degradation than the top, where the effect is not so clear). The low oxygen availability and rapid kinetics also meant that the oxidation almost immediately became oxygen-starved at the top of the bundle, and the starvation front migrated down to near the bottom of the heated length. Trial calculations in which the argon flow was increased up to 8.3 g/s (from 3 g/s simulating no effect of the cooling effects of the nitrogen in the air, and 4.3 g/s including this effect) reduced the rate of escalation to some extent, but did not materially affect the behaviour.

Following discussion between FZK and PSI specialists it was decided to reduce the power by about half at the end of the pre-oxidation phase and allow cool-down to about 1150 K before initiating the air ingress, in order to provide a longer period of air ingress and also to reduce the excessive extent of the starvation region. As a general advantage, bundle temperatures before air ingress are in this way closer to reactor conditions. Calculations were performed again with S/R5 and MELCOR using the revised boundary conditions as illustrated in Tab. 6.1 and Tab. 6.2. The cladding temperatures decrease sufficiently quickly at the nominal end of the pre-oxidation phase (Fig. 6.5) that they essentially re-stabilise within 2000 s, and the additional oxidation during that period is minimal. In this case the main cause of the initial temperature escalation in the subsequent phase is the reduced heat transfer conditions due to the change in flow rate and composition. As the temperatures rise, however, the heat release due to oxidation in air begins to dominate the escalation at the top of the bundle, and leading to region of oxygen starvation which progressively extends down toward the mid-section. The temperature increase is much slower, and the extent of the starvation region much less than was the case with air ingress initiated from the higher temperature.

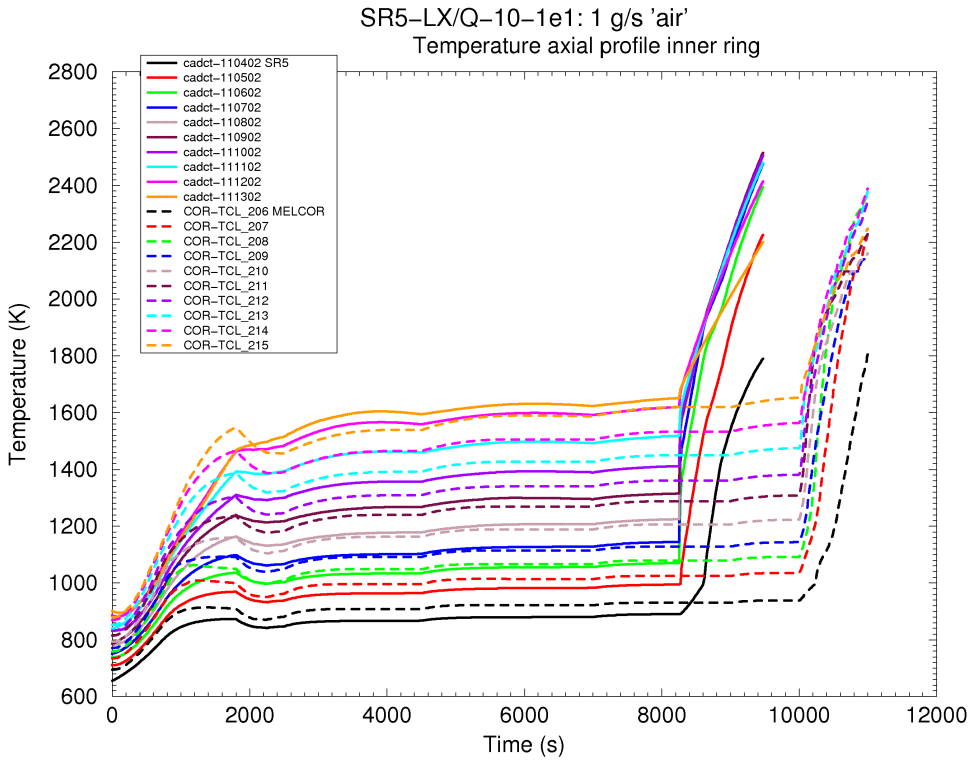

Fig. 6.1: PSI: MELCOR and S/R5 temperature histories, original specification

Comparison of temperature histories calculated for inner heated rods.

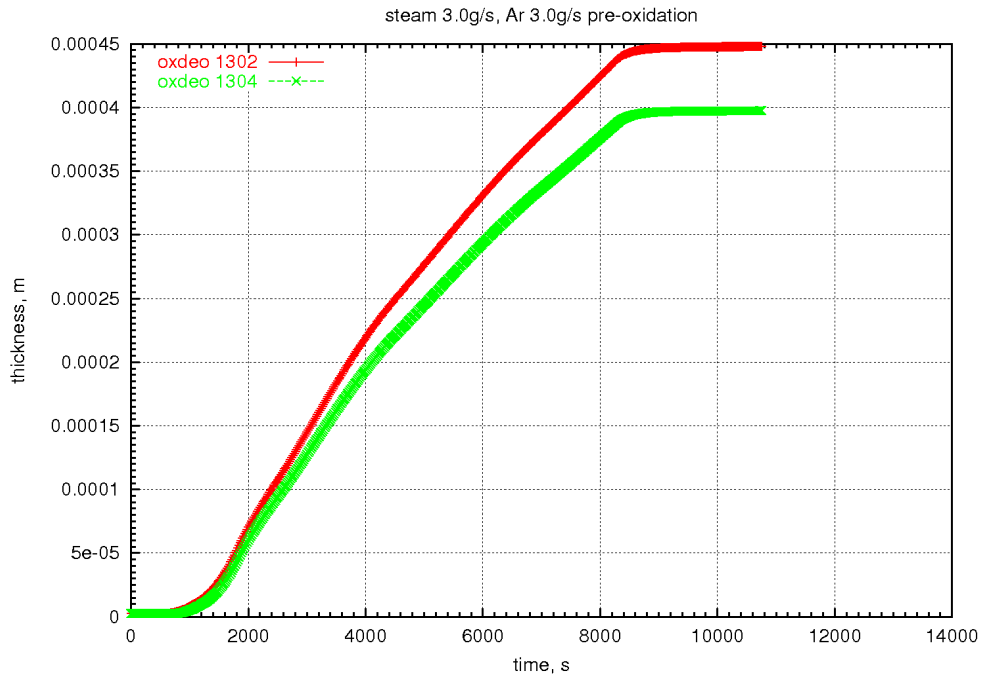

Fig. 6.2: PSI: Calculated peak reacted metal layer histories

The figure shows S/R5 results for inner heated rods (02) and corner rods (04). The temperature was reduced by a power reduction after required oxide thickness was attained.

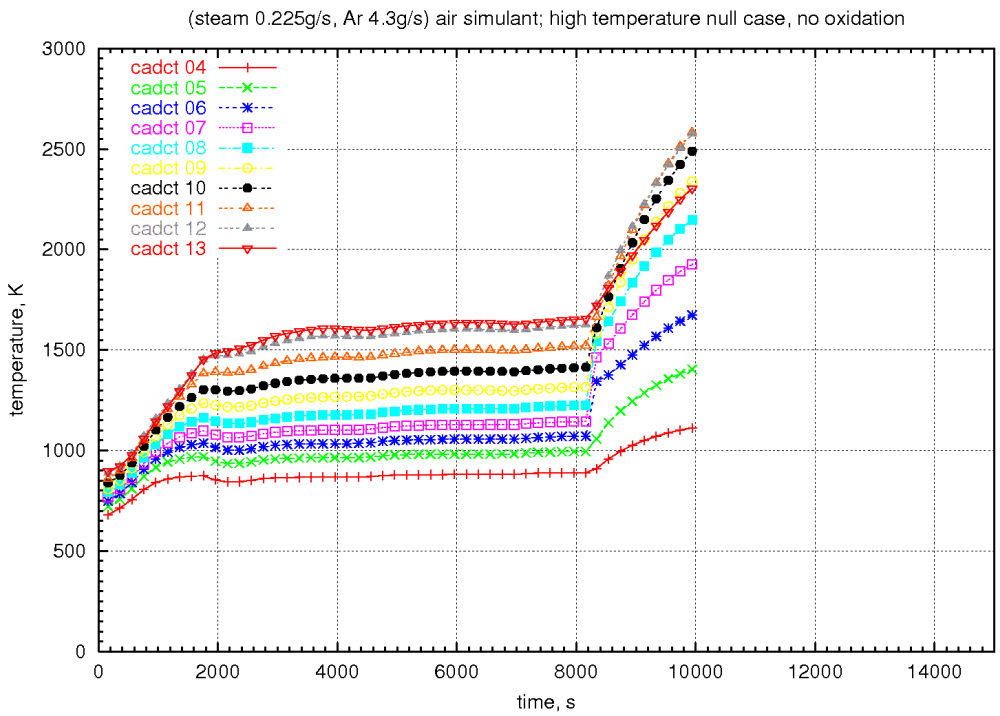

Fig. 6.3: PSI: Effect of reduced heat transfer only

The figure shows inner heated rod temperature histories, calculated by S/R5.

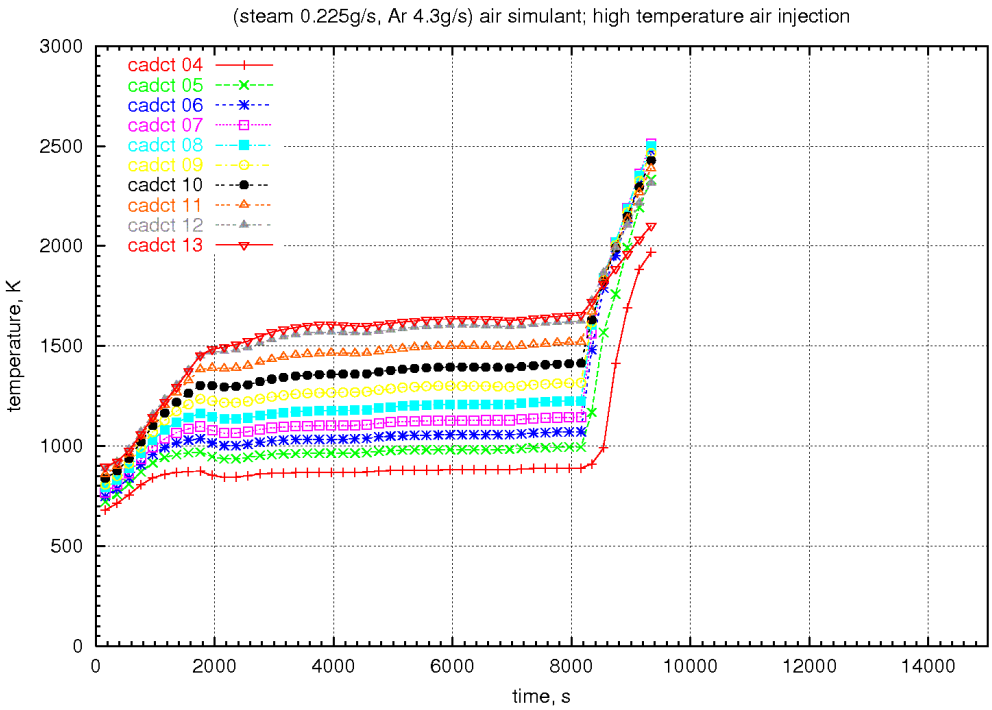

Fig. 6.4: PSI: Effect of reduced heat transfer and air oxidation

The figure shows inner heated rod temperature histories, calculated by S/R5.

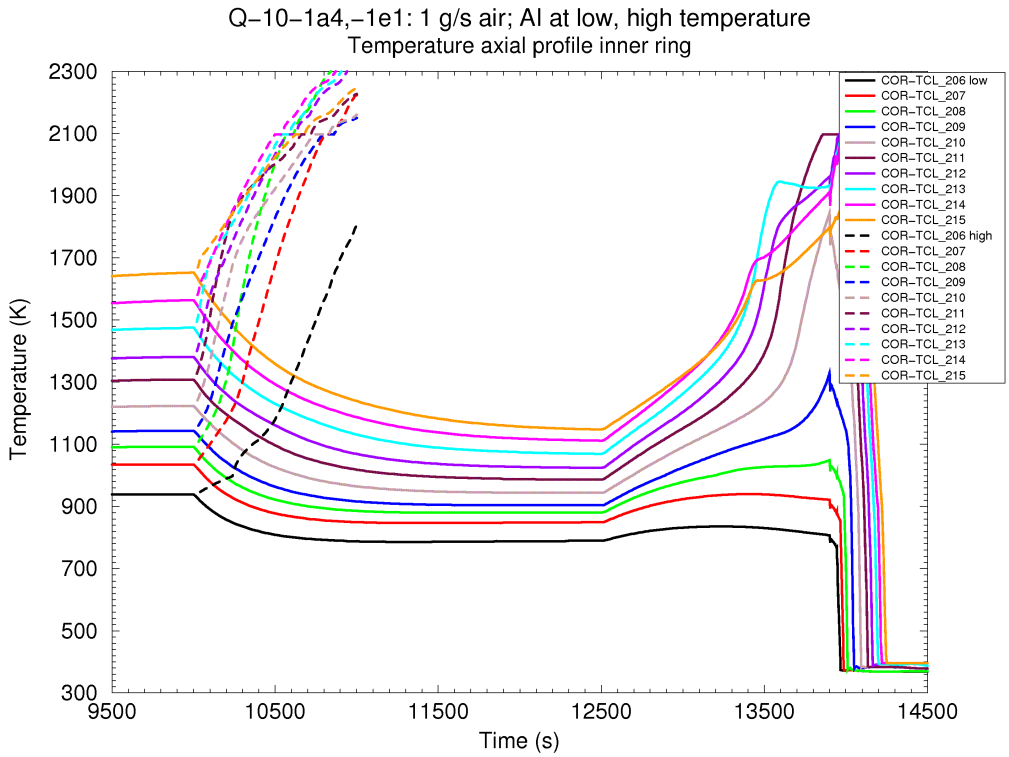

Fig. 6.5: PSI: MELCOR temperature histories, original and revised specification

Results refer to heated rods. For the revised specification, electrical power is decreased at the end of oxidation phase.

6.3 Quench/Cool-Down

Based on a maximum measured temperature of 2073 K (i.e. 1800 C) for initiation of either cool-down in an inert gas or reflood with water, a criterion of 2100 K was used in the calculations. Information provided by FZK indicated that the preferred method is reflooding at a flow rate yet to be specified, but the cool-down with inert gas was still under consideration at the time. In view of this uncertainty and the possibility of an oxidation excursion, alternative scenarios were investigated.

MELCOR calculations were performed for reflood at water injection rates of 20 g/s and 50 g/s, in each case following rapid refilling of the lower volume (as was performed in QUENCH-06), and also cool-down with 5 g/s helium and 50 g/s argon (i.e. the same molar flow). The heating power is reduced to ca. 4 kW for reflood, to simulate decay heat, and the same power was used in the calculations with cooling with inert gas. In this way the cooling effects could be compared directly, other inputs being the same, and also the rate of reflood, and choice of inert cooling medium. S/R5 calculations were performed for argon cooling at 30 g/s, and for water cooling at 20 g/s and 50 g/s. It was not possible to simulate cooling with helium with the current programme version. Numerical problems encountered during the quench phase, manifested as large mass errors, could be overcome to a certain extent by the artificial injection of a very small amount of argon during this period.

The MELCOR calculated temperatures at the top of the bundle with the different modes of cooling are shown in Fig. 6.6. All the cases demonstrate the bundle is finally cooled to ambient over a period of several minutes. This is achieved earlier in the case of reflood quench, although the initial cooling at the top of the bundle is slower, due to resumption of oxidation. The predicted reflood excursion is minimal at the higher injection rate, since the decay heat removal is re-established much earlier. The cool-down rates with helium and argon are comparable, as might be expected, as the molar flows are the same, though with overall faster cooling by helium, which is the more efficient heat transfer medium. The difference in cooling progression between reflood and inert gas is shown in more detail in Fig. 6.7. A similar picture was found for the S/R5 calculations, see Fig. 6.8 for 30 g/s argon cooling. It is noted that the gas cooling induces a concave temperature profile with time, while that for reflood cooling is convex. At all levels the reflood cooling with water accelerates as the bundle is progressively refilled, and then quenches. The refilling and quench front progression are shown as calculated with MELCOR in Fig. 6.9 and Fig. 6.10 for injection rates of 20 g/s and 50 g/s. At the faster rate the bundle fills quickly enough to establish almost immediate cooling, even though the quench front lags significantly behind. At the slower rate the re-establishment of cooling is delayed until sufficient water has been injected.

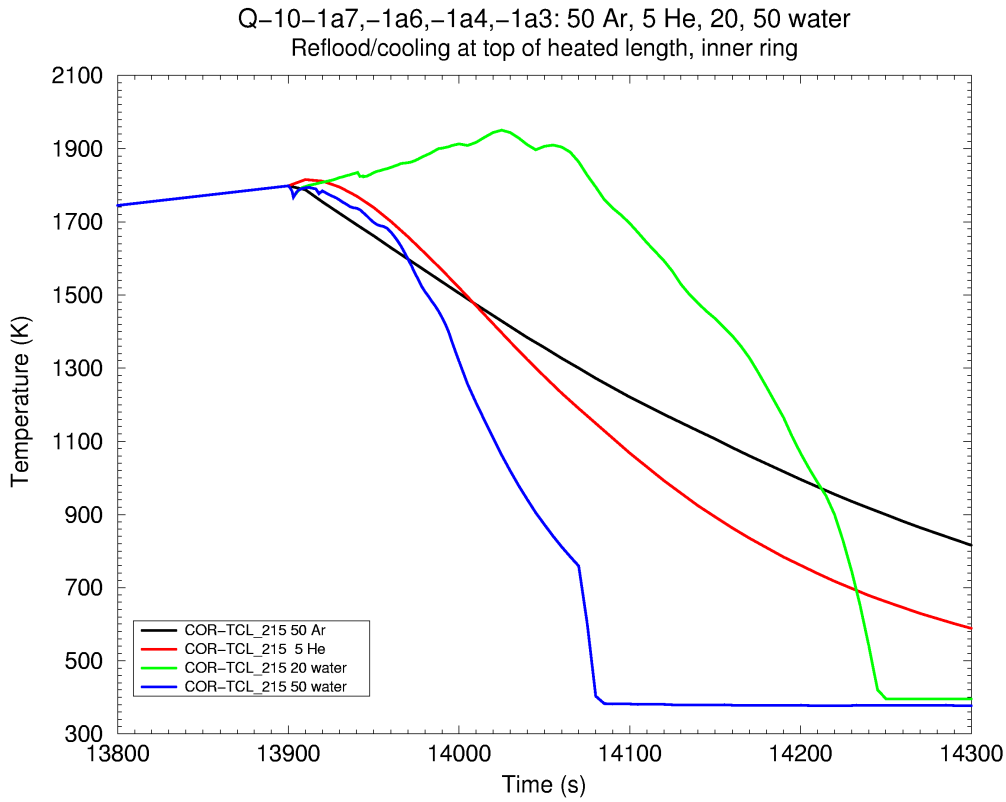

Fig. 6.6: PSI: Temperature histories for different cooling methods after air ingress

Results refer to heated rods, calculated with MELCOR.

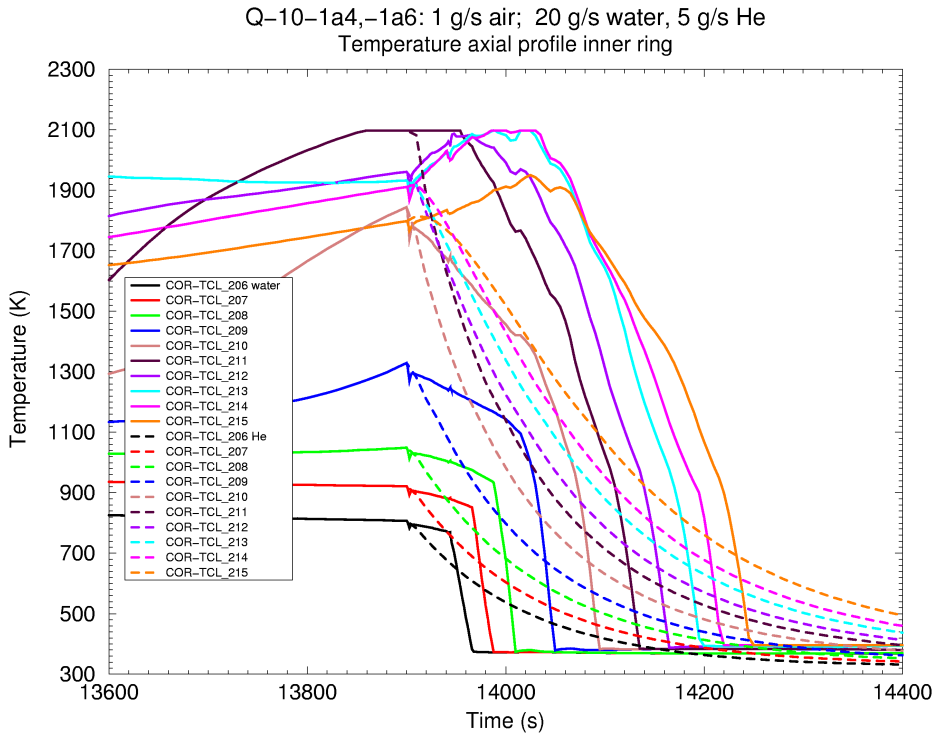

Fig. 6.7: PSI: Comparison of helium cooling and water quench (MELCOR)

Inner heated rod temperature histories for helium cooling 5 g/s and water quench (20 g/s).

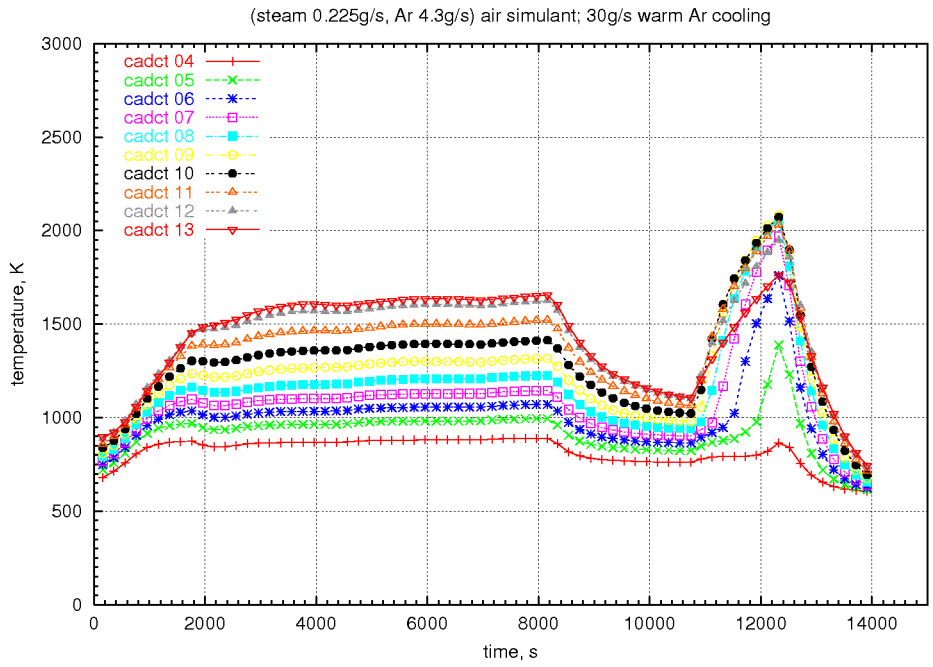

Fig. 6.8: PSI: S/R5 temperature histories for argon cooling at 30 g/s

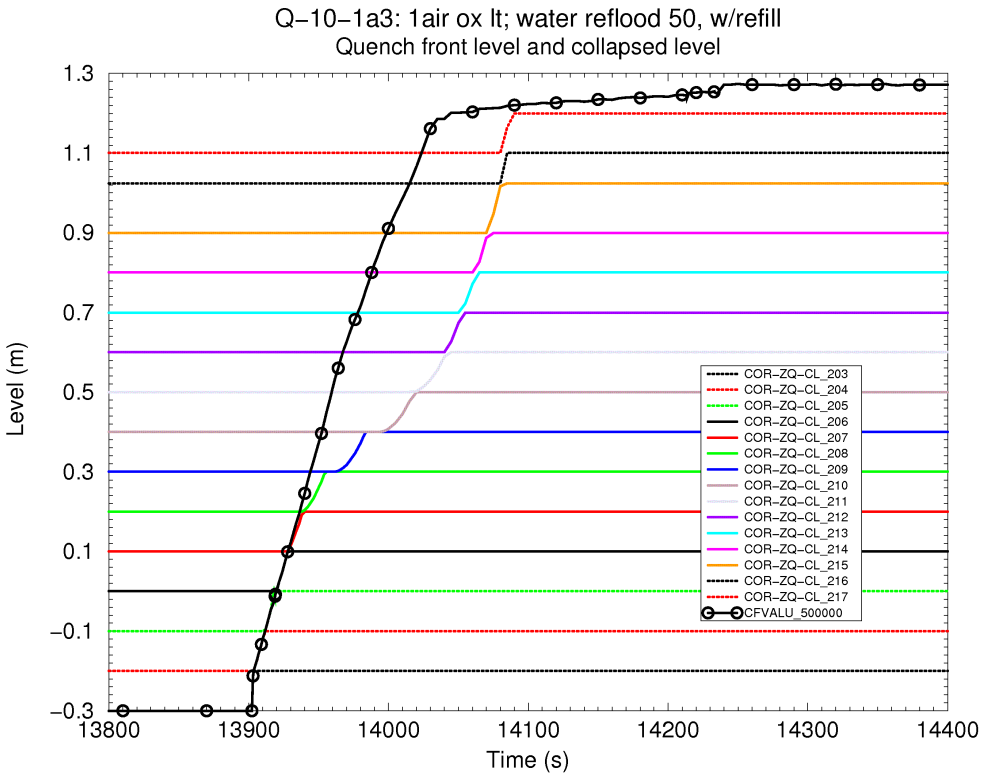

Fig. 6.9: PSI: Quench front and collapsed water level for water quench at 50 g/s

The results are calculated with MELCOR.

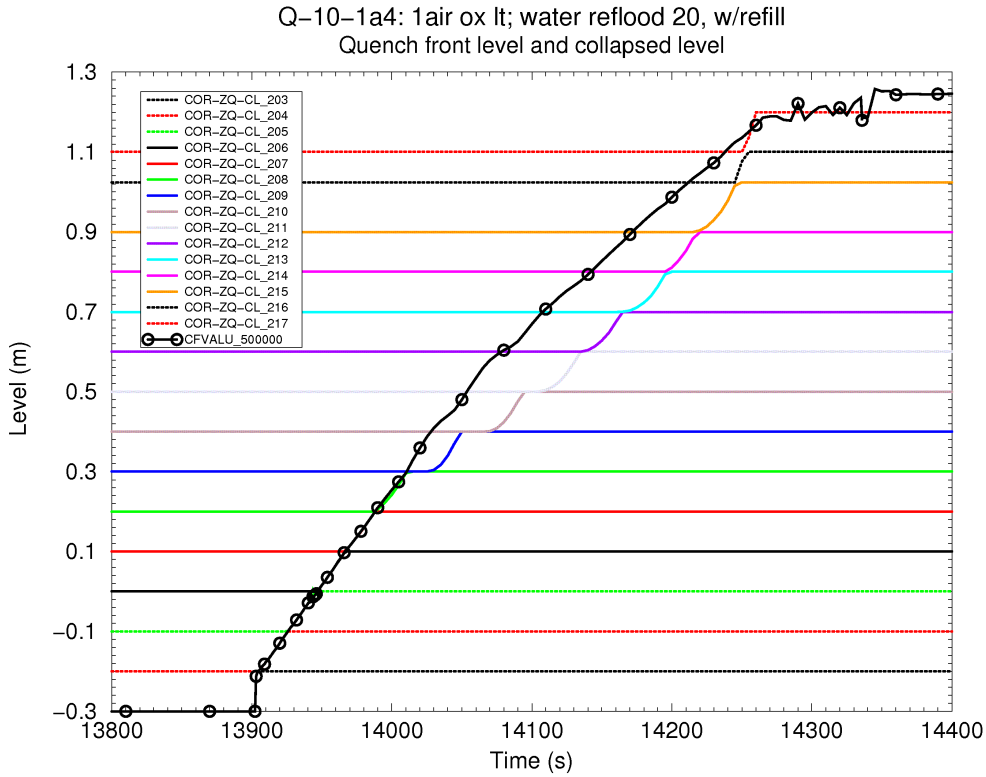

Fig. 6.10: PSI: Quench front and collapsed water level for water quench at 20 g/s

The results are calculated with MELCOR.

6.4 Oxidation

Fig. 6.11 and Fig. 6.12 show the oxidation transient calculated with MELCOR assuming reflood at 20 and 50 g/s, in terms of the mass of oxidised Zircaloy, and the mass of hydrogen generated. The oxidation increases rapidly during the initial temperature power ramp and then drops to a nearly steady rate as the quasi-plateau is established, then almost stopping when the power is reduced. In the period before air injection there is excess steam and the oxidation rate is kinetically limited. During the period of air injection the oxidation is limited by the small availability of oxygen, and of course no hydrogen is generated. The presence of nitrogen is not taken into account directly, neither as regards the formation of nitride nor as regards the interaction of nitrogen with the oxide layer – i.e. increasing the permeability or possibly flaking off the oxide shell. It is not clear how the lack of representation of these processes might affect the behaviour during air injection. However, there is an oxygen-starved region at high temperature where one might expect conditions to be conducive to nitriding as well as modification of the oxide shell. The calculations indicate a significant oxidation excursion during reflood at 20 g/s water injection, but less at 50 g/s. This is illustrated also in the S/R5 results shown in Fig. 6.13. Note that here the 'hydrogen' generated in the period from about 10500 s to about 12400 s, viz. the air ingress phase, is purely an artefact of the fact that steam has been used to simulate the air. Removing this, the agreement between the two codes is acceptable.

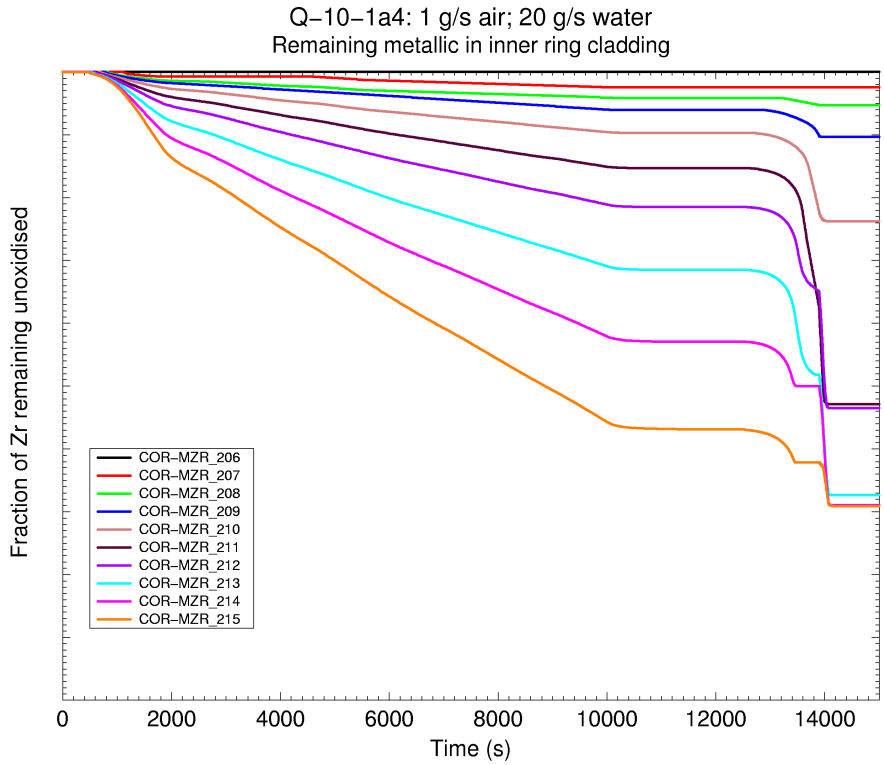

Fig. 6.11: PSI: Remaining metallic in inner ring cladding for water quench at 20 g/s

The results are calculated with MELCOR.

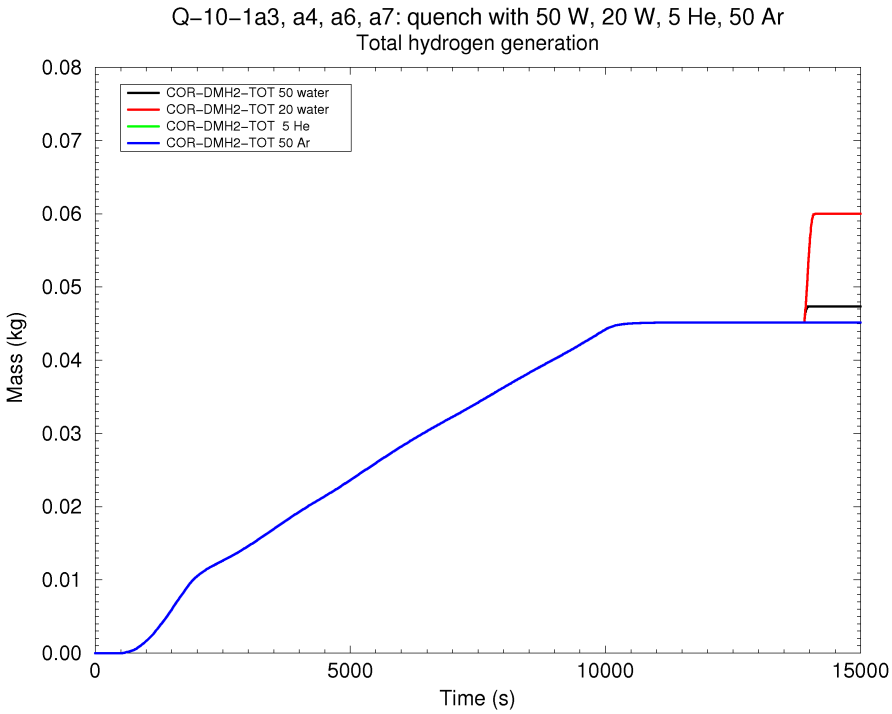

Fig. 6.12: PSI: Hydrogen production for different cooling methods

Results are calculated with MELCOR.

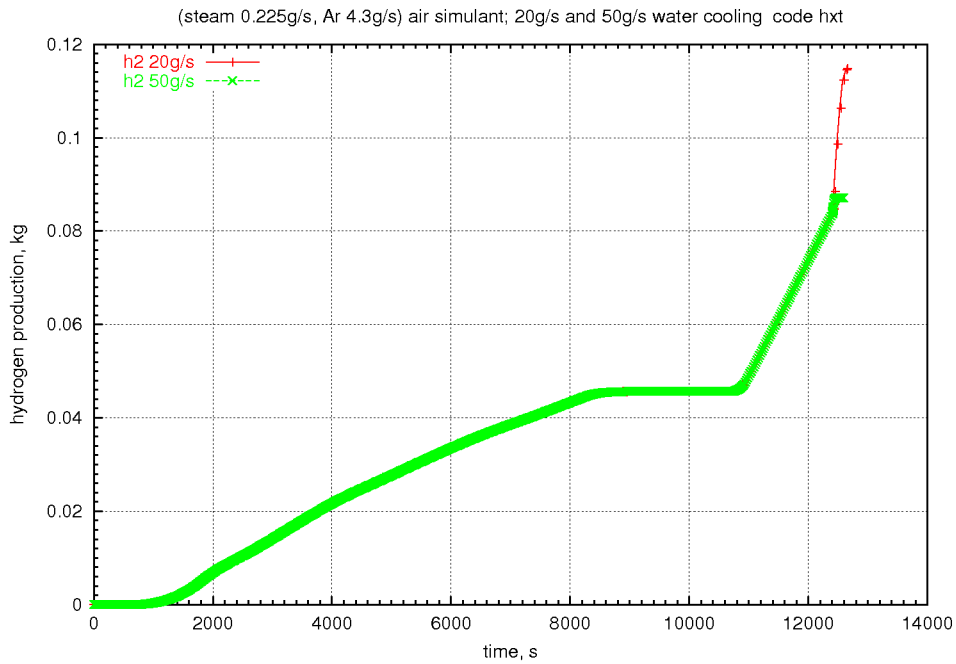

Fig. 6.13: PSI: Hydrogen production for reflood at 20 g/s and 50 g/s

The production between 10800 s and 12500 s should be ignored; it results from the simulation of air by steam (S/R5 calculation)

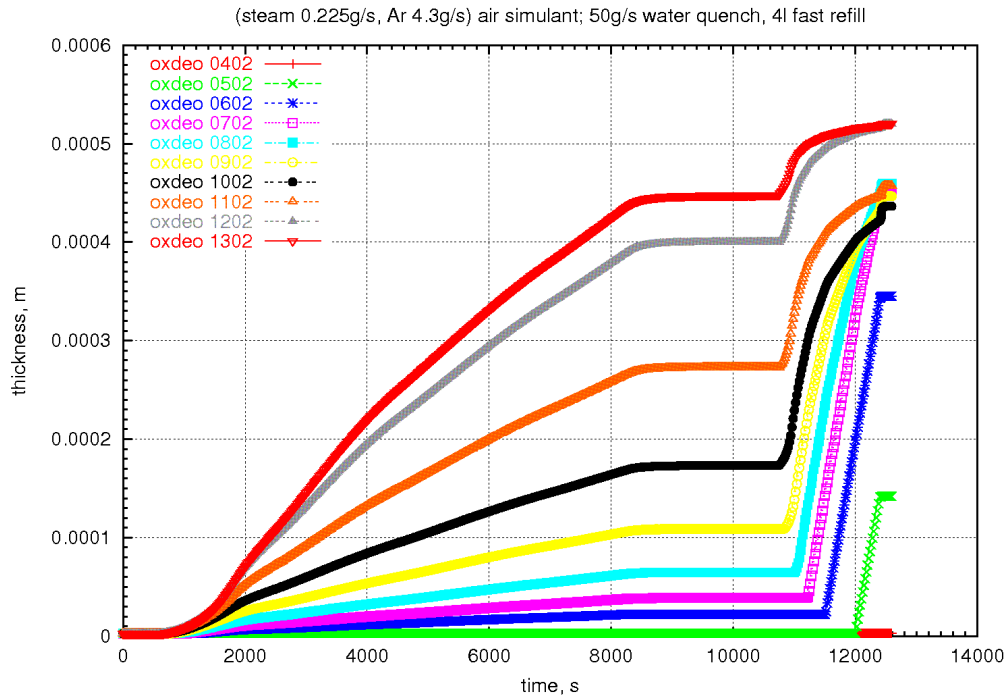

Fig. 6.14: PSI: Oxidised metal thickness for reflood at 50 g/s

The results, calculated by S/R5, show the effect of oxygen starvation in the air phase.

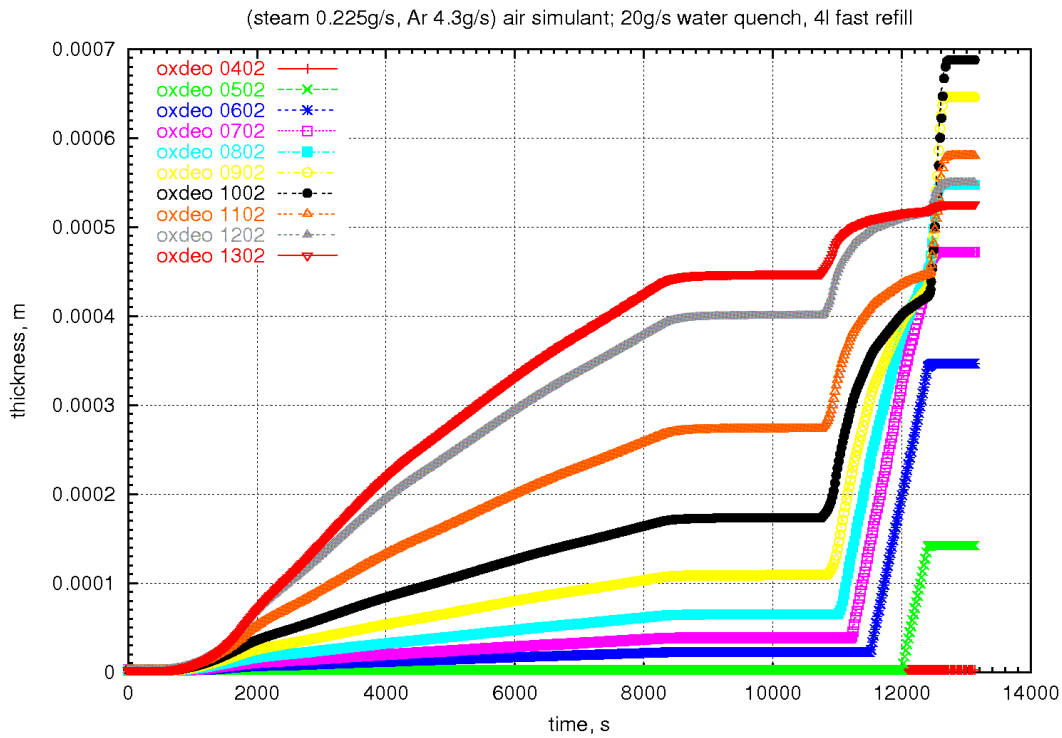

Fig. 6.15: PSI: Oxidised metal thickness for reflood at 20 g/s

The results, calculated by S/R5, show the effect of oxygen starvation in the air phase and localised excursion during quench.

The starvation effect is illustrated in Fig. 6.14 and Fig. 6.15 for water quench at 50 g/s and at 20 g/s. In the pre-oxidation phase, the temperature is higher at the top of the bundle, an effect resulting from the convective heat transfer and the well-known positive temperature coefficient of resistivity of the tungsten heaters. In the oxygen-starved air phase, with higher oxidation rates and heat of reaction than in steam, oxidation proceeds more rapidly at the lower elevations and leaves less oxygen available at the top. The effect of air ingress is to even out the axial oxidation profile.

6.5 Code Comparison and Discussion of Uncertainties

The calculations show a broadly similar thermal-hydraulic response, with some differences in the time for the pre-oxidation. The faster oxidation predicted by S/R5 appears to be attributable to the slightly higher temperatures; these are a result of the relative heat inputs and removal pathways, which are somewhat uncertain and modelled differently in the two codes. In any case a period of 9000 s would seem to be sufficient to provide the desired pre-oxidation.

Initiation of the air injection directly at the end of pre-oxidation would be problematic, resulting in a rapid excursion and oxygen starvation throughout almost the entire heated length. A period of reduced power and cooling to ca. 1150 K will allow the oxidation excursion to develop progressively as the bundle heats up again, following an initial temperature increase due to the reduced heat transfer afforded by 1 g/s air compared with 3 g/s steam. The test protocol allows for the possibility of increasing the power if the excursion is too weak, but the calculations suggest this will not be necessary. This protocol is similar to that used in the CODEX-AIT2 test [1].

There is some uncertainty about the rate of air oxidation. While the total rate of oxide formation is controlled by the availability of oxygen, the presence of nitrogen may affect the morphology of the oxide shell, reducing its resistance to transport of oxygen and possibly to early breakaway if a nitrogen-bearing layer forms underneath, leading possibly to local oxidation peaks. There is also the possibility of zirconium nitride formation, with attendant chemical and mechanical effects (such as possible breakaway alluded to in the previous sentence), and a limited amount of reaction heat. Neither code is able to treat these effects changes. It is noted that extensive zirconium nitride formation was observed in CODEX-AIT1 and AIT2 [1].

There is some likelihood of an oxidation excursion during reflood. The calculations suggest this is more likely at a lower injection rate. Although only a very minor oxidation is predicted at an injection rate of 50 g/s, a significant excursion remains a possibility. The predictions take no account of the effect of previous exposure to air, and so the excursion might be underestimated in one or both cases. In addition, experience from previous QUENCH experiments suggest that starvation in the previous period, near the top of the bundle, might cause the cladding to be in a more flammable state due to redissolution of the oxide shell beta-Zircaloy. The effect of starvation history is not taken into account in the models available in the code used. Finally, in the case of significant nitriding, there is also the possibility of an energetic reaction between zirconium nitride and water, and release of resulting gases.

Overall, there was a clear advantage in using two independent codes to calculate the expected response, as each code has different strengths and weaknesses. It is reassuring that similar results were obtained in each case, notably only differences in timing were apparent. The conclusions drawn regarding test conduct were the same whichever code was taken as the basis.

7 End of Pre-Oxidation Phase

The partners, involved in QUENCH-10, agreed that pre-oxidation should end, when the maximum oxide scale in the bundle (i.e. of the inner heated rods) is 600 µm. However, the experimental team cannot measure the oxide scale continuously during the test, and least at all its maximum value. Withdrawal of a corner rod gives only one current state, and it is quite uncertain that it just corresponds to the desired value for the inner rod. Besides, oxidation continues in the bundle, while the scale of the withdrawn rod is measured, so that the value of this information would be rather small. In addition, experience shows that for one reason or another a test differs somewhat from the pre-test calculations. Therefore, the pre-oxidation phase cannot be ended at the time that is predicted in these calculations, and another solution has to be found.

The only information about oxidation that is available continuously during the test is the cumulated hydrogen generation in the bundle. Pre-test calculations give both cumulated hydrogen generation and maximum oxide scale for every time step, and we propose to correlate cumulated hydrogen production and maximum oxide scale from the pre-test calculations and apply this correlation during the test. Strictly speaking, cumulated hydrogen mass is an integral value, whereas maximum oxide scale is a local information, and there is no unique correlation between these two values. Since, however, the temperature profile is well known and rather fixed during the pre-oxidation (Fig. 4.5), the relation between the maximum oxide scale and cumulated hydrogen production in the bundle, deduced from the pre-test calculations, should not be too far from reality for QUENCH-10.

All calculated information to this aspect from S/R5, MELCOR, and SVECHA results is collected in Fig. 7.1. Original MELCOR results refer to the depth of oxidised metallic Zr assuming no additional processes as thermal expansion, strain, or alpha-layer take-up. Therefore, to estimate the oxide scale, original MELCOR results are multiplied by 1.5, corresponding approximately to the PB ratio. SVECHA results are extrapolated to bundle conditions, assuming a constant lateral temperature profile. Including experimental data of previous QUENCH tests proved not to be helpful.

S/R5 and MELCOR results increase nearly linearly. For S/R5, this is compatible to the observation about total hydrogen production in the rod and hydrogen production at axial elevation 0.925 m, as discussed earlier. In contrast, SVECHA results increase faster than linearly with accumulated hydrogen generation. S/R5 results from PSI are quite close to FZK results, demonstrating that the codes and the input data are quite similar. MELCOR results give a somewhat higher maximum oxide scale than SVECHA results. This is credible, because MELCOR results refer to the inner heated rods and SVECHA results to the unheated central rod.

For a maximum oxide scale of 600 µm at the end of the pre-oxidation phase, aimed in the test, SVECHA predicts about 28 % less cumulated hydrogen production for the central rod than S/R5. MELCOR calculations predict about 32 % less cumulated hydrogen production than FZK S/R5 calculations for the inner heated rods. For the same maximum oxide scale of 600 µm, the difference of cumulated hydrogen production between MELCOR and SVECHA

results are similar to that for FZK S/R5 calculations for the two rod types. This suggests that MELCOR results for the central rod should be close to SVECHA results. Taking in mind the error in S/R5 for thick oxide scales, the comparison of the various computational results suggests to stop pre-oxidation, when 44 g hydrogen are produced in the bundle since the start of the test. Hydrogen production rate (Fig. 5.1) is limited so that the time interval for this decision is not critical.

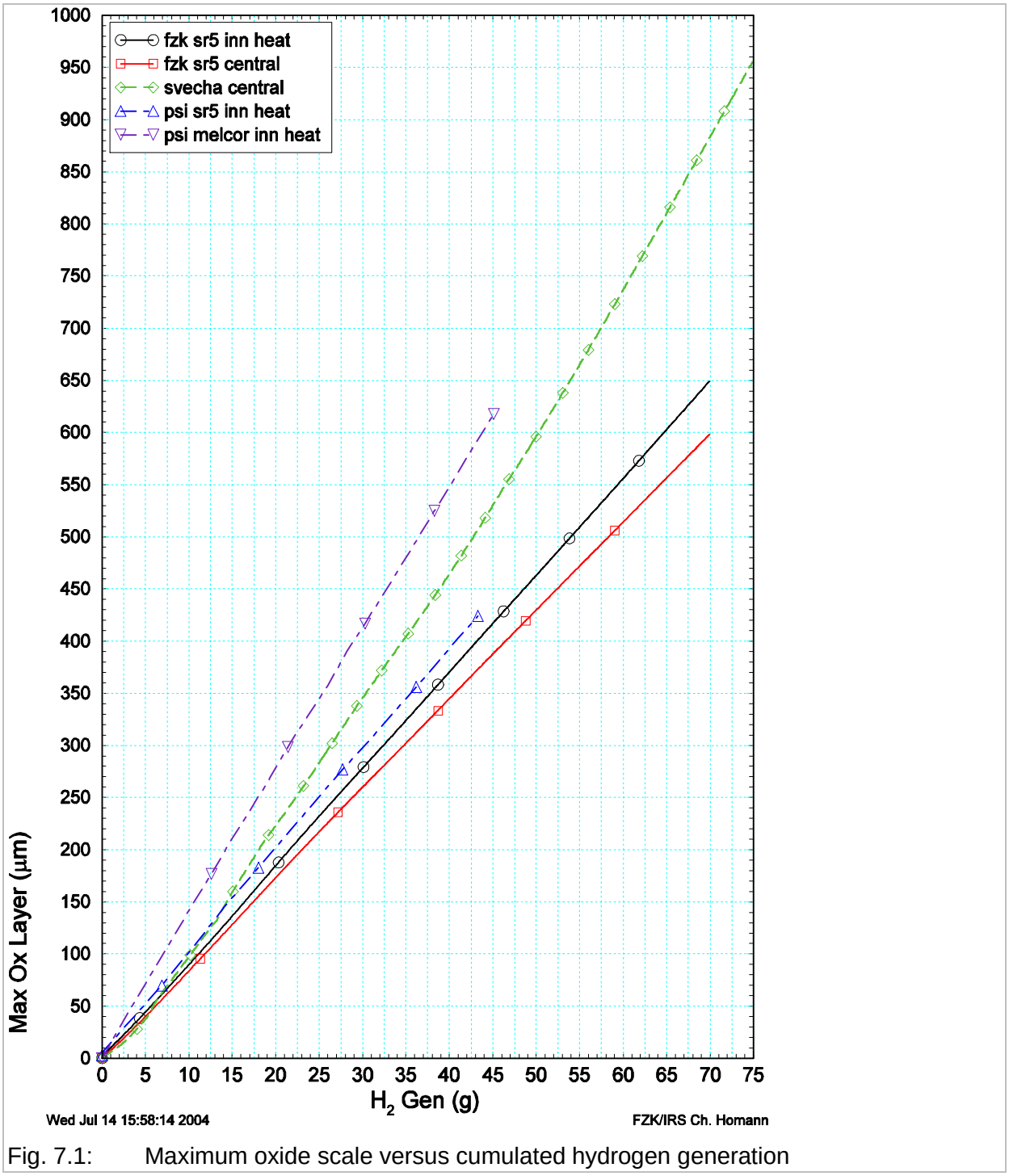

Fig. 7.1: Maximum oxide scale versus cumulated hydrogen generation

The figure shows all available results for the central and the inner heated rods as calculated with MELCOR, S/R5 and SVECHA

8 Joint Proposals for Final Test Protocol

In sum, the following proposals were derived from the joint analytical work. Up to air ingress phase, the test should be run with 3 g/s steam and argon each. Temperature rise in the first transient should be faster than in QUENCH-09 to reach the temperature plateau rather fast, but not faster than in QUENCH-05 to limit thermal loads in the rods.

During pre-oxidation phase, maximum bundle temperature should be kept below about 1600 K as long as the oxide scale is small to avoid a temperature escalation. Then pre-oxidation should be performed such that hydrogen production rate is constant, as proposed in QUENCH-01 and used since then; a value of about 5 mg/s being suggested. This test conduct implies that electrical power is increased, when the hydrogen production rate falls below a certain value, say 4.5 mg/s, and that temperature increases with time. In both S/R5 and MELCOR calculations, maximum temperature is predicted to increase to about 1700 K under such conditions. This test conduct is proposed for two reasons. Firstly, hydrogen production rate is a more sensible measure than temperature and therefore a more efficient way to control the test. Secondly, it gives by far a shorter pre-oxidation phase, reducing work and stress of operators, consumption of argon, and the amount of experimental data.

Before air ingress starts, the bundle should be cooled down to about 1150 K, preferably by reducing electrical power, to reduce subsequent temperature rise and hence to get more information during air ingress. Additional oxidation during this intermediate cool-down is very small, because temperature and hence oxidation are predicted to decrease rather fast. If the predicted temperature increase during air ingress proves to be smaller in the test than calculated, electrical power should be increased stepwise. As a second advantage, test conditions are in that way closer to CODEX-AIT experiments.

During the test, the maximum bundle temperature and its derivative with respect to time should be compared to predicted values during intermediate cool-down and air ingress phase to optimize the test conduct. For earlier test phases this procedure is not necessary due to the operators' experience.

Withdrawal of the two corner rods should be performed at about the end of pre-oxidation and at about the end of air ingress phase to have maximum information for the air ingress phase, taking in mind that during air ingress and quench phase quantitative information is scarce, especially from bundle TCs in the hot region after the long pre-oxidation phase. Not only the start, but also the end of withdrawals should be carefully noted to facilitate interpretation if difficulties arise to withdraw the corner rods.

After controversial discussion about the various possibilities it was decided by FZK specialists to quench the bundle with water as final test phase, but with the elevated injection rate of 50 g/s. Though this is not as prototypical as it is desirable, this solution was preferred to reduce the risks of an extended temperature excursion, above all damage of the facility, but also of contributions of non-prototypical components, e.g. strong oxidation of electrode material.

9 Conclusions

Test QUENCH-10 is dedicated to study air ingress with subsequent water quench during a supposed accident in a spent fuel storage tank, based on a scenario proposal by AEKI, Budapest. Since it is the first test on air ingress in the QUENCH facility, more analytical work was necessary for its preparation, though the nuclear scenario had been simplified. For this purpose, the successful cooperation between Paul Scherrer Institut and Forschungszentrum Karlsruhe was continued, and the related work relied on more than one severe accident codes, namely on the two codes SCDAP/RELAP5 and MELCOR. Though the respective code models are significantly different, comparison of the results shows that both codes give broadly similar results for the same nominal boundary conditions and helped to assess the sensitivity of the facility.

For pre-oxidation, a steam mass flow rate of 3 g/s, as used in previous tests, was seen to be preferable to a smaller value. The hydrogen production rate should be kept at a more or less constant value of about 5 mg/s so that the duration of that phase keeps within acceptable limits. To reach the requested maximum oxide scale of 600 µm in the bundle at about 1600 K before air ingress, MELCOR predicted a duration of the pre-oxidation phase of about 10000 s leading to the generation of about 44 g hydrogen. Temperatures, calculated with S/R5, are slightly higher than with MELCOR. Comparison of the respective results and additional work with SVECHA and separate effects tests, both performed by the experimental group, revealed an error in S/R5, suggesting that thick oxide scales are underestimated. The combined effort of the involved partners was used to derive a criterion, when the requested oxide scale is reached in the test, because that information is not available on-line.

To describe air ingress, modelling in MELCOR is more advanced than in S/R5, but nitride formation is not included in any of these codes. For the preparation of QUENCH-10, oxidation kinetics and heat of reaction were modified in S/R5, but modelled gas composition (hydrogen, steam) is not representative for experimental conditions. With these restrictions, both codes predict a rapid excursion due to air ingress and oxygen starvation in upper and middle parts of bundle. The starvation front propagates to near bottom of heated section; the maximum temperature rise rate is about 4 K/s. Further work showed that pre-cooling to about 1150 K reduces the rate of excursion and moderates downward propagation of the starvation front. Alternatively, an increase of argon flow rate to 8.3 g/s would be possible, but this is not so efficient. A suitable power reduction and bundle cooling makes the air ingress phase easier to control and interpret and is therefore recommended for the test conduct. Besides, test conditions are in that way closer to CODEX-AIT experiments.

Since at that time final decisions were not yet taken, cool-down with inert gas and water quench were investigated. It was found that water quench implies the risk of temperature excursion, but is more representative of the accident conditions in a spent fuel storage pool. Significant additional hydrogen generation is predicted at lower (20 g/s) water injection rate, less at 50 g/s because of higher heat transfer rates and smaller cooling time. For these two cases, the lower injection rate would be more representative for the envisaged accident scenario in the spent fuel storage pool, but the higher injection rate would give faster temperature decrease. However, there is a large uncertainty in the magnitude of excursion. It might

be larger than predicted, because in the preceding air ingress phase the upper region of bundle has been oxygen starved, and the oxide scale is expected to be reduced for this reason. Furthermore, the effect of water on zirconium nitride cannot be quantified due to lacking code models, but is expected to result in increased hydrogen production. In contrast, for cool-down in argon or helium, the cool-down rate is controllable by selection of gas and injection rate. Helium results in faster cooling at same molar flow than argon.

In sum, the code predictions suggest that water quench is likely to result in mechanical damage to bundle, and this effect has impacts on post test examination of the bundle and interpretation of the experimental results. Cool-down in inert gas would avoid the problem of temperature excursion and reduce damage, but it is not prototypic of the conditions in the spent fuel storage pool and it would not be representative for reactor conditions either.

Furthermore, improvements of the experimental set-up and the test conduct were suggested and largely applied. In SCDAP/RELAP5 an error was found concerning the output value of oxide scale for heavy oxidation. For the aims of the test preparation its consequences could be taken into account.

10 Acknowledgement

The test QUENCH-10 and the related computational support were co-financed as test QUENCH-L1 by the European Community under the Euratom Fifth Framework Programme on Nuclear Fission Safety 1998 – 2002 (LACOMERA Project, contract No. FIR1-CT2002-40158).

We thank the experimental group at IMF for their contributions to this report and Dr. Z. Hózer for communicating details of the nuclear scenario.

11 References

[1] Shepherd I., Haste T., Kourti N., Hummel R., Oriolo F., Leonardi M, Knorr J., Buchmann M., Gleisberg O., Kaltofen R., Schneider R., Hofmann P., Schanz G., Plitz H., Adroguer B., Chatelard P., Roche S., Hózer Z., Maróti L., Matus L., Windberg P.: Oxidation Phenomena in Severe Accidents (OPSA) - Final Report, INV-OPSA (99)-P008, EUR 19528 EN, April 2000.

[2] Miassoedov, A., Alsmeyer, H., Eppinger, B., Meyer, L., Steinbrück, M.: Large scale experiments on core degradation, melt retention and coolability (LACOMERA). FISA-2003, EU Research in Reactor Safety; Conclusion Symp. on Shared-Cost and Concerted Actions, Luxembourg, L, November 10-13, 2003, Luxembourg, Office for Official Publications of the European Communities, 2004, pp. 373 – 378, EUR-21026, ISBN 92-894-7803-9.

[3] Homann, Ch., Hering, W., Birchley, J., Fernandez Benitez, J. A., Ortega Bernardo, M.: Analytical Support for B_4C Control Rod Test QUENCH-07, Forschungszentrum Karlsruhe, FZKA 6822, SAM-COLOSS-P055, Karlsruhe, April 2003.

[4] Hózer, Z.: Spent Fuel Storage Pool Accidents: the Scenario behind QUENCH-10 Experiment, 10th International QUENCH Workshop, Forschungszentrum Karlsruhe, October 26-28, 2004.

[5] Lipar, M. et al.: Report of the Expert Mission ‘To Assess the Results of the Hungarian Atomic Energy Authorities Investigation of the 10 April 2003 Fuel Cleaning Incident at Paks NPP’, Hungarian Atomic Energy Authority and Paks Nuclear Power Plant Hungary, conducted under IAEA Technical Co-operation Project HUN/9/022, Support for Nuclear Safety Review Mission, 16 to 25 June 2003.

[6] Hering, W., Homann, Ch., Lamy, J.-S., Miassoedov, A., Schanz, G., Steinbrück, M., Sepold, L.: Comparison and Interpretation Report of the OECD International Standard Problem No. 45 Exercise (QUENCH-06), Forschungszentrum Karlsruhe, FZKA 6722, July 2002.

[7] The SCDAP/RELAP5 Development Team: SCDAP/RELAP5/MOD 3.2 Code Manual, NUREG/CR-6150, INEL-96/0422, Idaho Fall, Idaho, USA, 1997.

[8] Sanchez, V., Elias, E., Homann, Ch., Hering, W., Struwe, D.: Development and Validation of a Transition Boiling Model for the RELAP5/MOD3 Reflood Simulation, Forschungszentrum Karlsruhe, FZKA 5954, Sep. 1997.

[9] Hering, W., Homann, Ch.: Improvement of the Severe Accident Code SCDAP/RELAP5 mod 3.2 with respect to the FZK QUENCH facility, Forschungszentrum Karlsruhe, FZKA 6566, to be published.

[10] Hofmann, P., Hering, W., Homann, C., Leiling, W., Miassoedov, A., Piel, D., Schmidt, L., Sepold, L., Steinbrück, M.: QUENCH-01 Experimental and Calculational Results, Forschungszentrum Karlsruhe, FZKA 6100, Nov. 1998.

[11] Frepoli C., Hochreiter L.E., Mahaffy J., Cheung F.B.: A noding sensitivity analysis using COBRA-TF and the effect of spacer grids during core reflood, ICONE-8711, Proceedings of ICONE-8, April 2-6, 2000, Baltimore, MD, USA, New York, ASME, CD-ROM.

[12] Homann, Ch., Hering, W.: Analytical Support for B_4C Control Rod Test QUENCH-09, Forschungszentrum Karlsruhe, FZKA 6853, SAM-COLOSS-P057, Karlsruhe, April 2003.

[13] Schanz, G., Forschungszentrum Karlsruhe: private communication, 19. Feb. 2004.

[14] Schanz, G., Hozer, Z., Matus, L., Miassoedov, A., Nagy, I., Sepold, L., Stegmaier, U., Steinbrück, M., Steiner, H., Stuckert, J., Windberg, P.: Results of the QUENCH-10 Experiment on Air Ingress, Forschungszentrum Karlsruhe, FZKA 7087, SAM-LACOMERA-D07, to be published.

[15] Hózer Z., Windberg P., Nagy I., Maróti L., Matus L., Horváth M., Pintér A., Balaskó M., Czitrovszky A., Jani P.: Interaction of Failed Fuel Rods under Air Ingress Conditions, Nucl. Technology, vol. 141 (2003) pp. 244-256.

[16] Hering, W., Forschungszentrum Karlsruhe: private communications to J. Birchley and T. Haste (Paul Scherrer Institut), March-April 2004.